

NASA/TM—2008–215250



# **Sulfur ‘Concrete’ for Lunar Applications— Environmental Considerations**

*R.N. Grugel*

*Marshall Space Flight Center, Marshall Space Flight Center, Alabama*

---

*February 2008*

## The NASA STI Program...in Profile

Since its founding, NASA has been dedicated to the advancement of aeronautics and space science. The NASA Scientific and Technical Information (STI) Program Office plays a key part in helping NASA maintain this important role.

The NASA STI program operates under the auspices of the Agency Chief Information Officer. It collects, organizes, provides for archiving, and disseminates NASA's STI. The NASA STI program provides access to the NASA Aeronautics and Space Database and its public interface, the NASA Technical Report Server, thus providing one of the largest collections of aeronautical and space science STI in the world. Results are published in both non-NASA channels and by NASA in the NASA STI Report Series, which includes the following report types:

- **TECHNICAL PUBLICATION.** Reports of completed research or a major significant phase of research that present the results of NASA programs and include extensive data or theoretical analysis. Includes compilations of significant scientific and technical data and information deemed to be of continuing reference value. NASA's counterpart of peer-reviewed formal professional papers but has less stringent limitations on manuscript length and extent of graphic presentations.
- **TECHNICAL MEMORANDUM.** Scientific and technical findings that are preliminary or of specialized interest, e.g., quick release reports, working papers, and bibliographies that contain minimal annotation. Does not contain extensive analysis.
- **CONTRACTOR REPORT.** Scientific and technical findings by NASA-sponsored contractors and grantees.

- **CONFERENCE PUBLICATION.** Collected papers from scientific and technical conferences, symposia, seminars, or other meetings sponsored or cosponsored by NASA.
- **SPECIAL PUBLICATION.** Scientific, technical, or historical information from NASA programs, projects, and missions, often concerned with subjects having substantial public interest.
- **TECHNICAL TRANSLATION.** English-language translations of foreign scientific and technical material pertinent to NASA's mission.

Specialized services also include creating custom thesauri, building customized databases, and organizing and publishing research results.

For more information about the NASA STI program, see the following:

- Access the NASA STI program home page at <<http://www.sti.nasa.gov>>
- E-mail your question via the Internet to <[help@sti.nasa.gov](mailto:help@sti.nasa.gov)>
- Fax your question to the NASA STI Help Desk at 301-621-0134
- Phone the NASA STI Help Desk at 301-621-0390
- Write to:  
NASA STI Help Desk  
NASA Center for AeroSpace Information  
7115 Standard Drive  
Hanover, MD 21076-1320

NASA/TM—2008–215250



# **Sulfur ‘Concrete’ for Lunar Applications— Environmental Considerations**

*R.N. Grugel*

*Marshall Space Flight Center, Marshall Space Flight Center, Alabama*

National Aeronautics and  
Space Administration

Marshall Space Flight Center • MSFC, Alabama 35812

---

***February 2008***

## **Acknowledgments**

The author is grateful to Professor H. Toutanji at The University of Alabama in Huntsville for his help and comments and to his group for providing sulfur concrete samples. Appreciation is also expressed to the Marshall Space Flight Center In Situ Fabrication and Repair Element of the In Situ Resource Utilization (ISRU) as well as Materials & Processes Laboratory EM30 for their support of this work. Appreciation is further expressed to Mr. Curtis Bahr for his technical expertise in supporting this work. A sincere appreciation is also extended to Ms. Linda Woolf for her critical reading of the manuscript.

The ISRU is a core component of the Vision for Space Exploration as implemented by the Science & Mission Systems (S&MS) Office. The ISRU works to establish, evaluate, and assess the in situ resources available on the Moon and Mars and the technologies needed to utilize and exploit these resources.

## **TRADEMARKS**

Trade names and trademarks are used in this report for identification only. This usage does not constitute an official endorsement, either expressed or implied, by the National Aeronautics and Space Administration.

Available from:

NASA Center for AeroSpace Information  
7115 Standard Drive  
Hanover, MD 21076-1320  
301-621-0390

This report is also available in electronic form at  
<<https://www2.sti.nasa.gov>>

## TABLE OF CONTENTS

1. INTRODUCTION .....	1
2. SUBLIMATION CONSIDERATIONS .....	4
2.1 Experimental Procedure .....	5
2.2 Experimental Results .....	8
2.3 Discussion of Sublimation Concerns .....	14
2.4 Summary of Sublimation Concerns .....	21
3. EXTREME COLD AND TEMPERATURE CYCLE CONSIDERATIONS REGARDING THE INTEGRITY AND COMPRESSION STRENGTH OF SULFUR CONCRETE .....	22
3.1 Experimental Procedure .....	22
3.2 Experimental Results .....	23
3.3 Discussion of Extreme Temperature Concerns .....	23
3.4 Summary of Extreme Temperature Concerns .....	31
4. OVERALL SUMMARY AND CONCLUSIONS .....	33
REFERENCES .....	34

## LIST OF FIGURES

1.	Eight-cubic-yard heater-mixer mobile production unit .....	1
2.	Pouring of Chempruf Sulfur Concrete in an industrial plant .....	2
3.	Chempruf Sulfur Concrete: acid containment system .....	2
4.	Precast Chempruf Sulfur Concrete tanks for Aqua Regia .....	2
5.	Typical unary sulfur phase diagram .....	4
6.	A piece of sulfur-based concrete made at The University of Alabama in Huntsville .....	5
7.	Photograph of the vacuum chamber used for the sublimation experiments .....	6
8.	Extrapolation of the solid-vapor transition line on a unary sulfur phase diagram .....	7
9.	Comparison of the sulfur concrete surfaces after vacuum processing of the upper right-hand corner section .....	7
10.	Surface morphology of the as-cast pure sulfur .....	8
11.	Surface morphology of the as-cast pure sulfur after vacuum processing on the order of $3-7 \times 10^{-6}$ torr ( $4-9.3 \times 10^{-4}$ Pa) for $\approx 11$ days .....	8
12.	Surface morphology of the as-cast pure sulfur after vacuum processing on the order of $3-7 \times 10^{-6}$ torr ( $4-9.3 \times 10^{-4}$ Pa) for $\approx 54$ days .....	9
13.	Sulfur - 65 wt. % JSC-1 samples subjected to vacuum processing .....	9
14.	Sulfur and silica binder mixture (25% sulfur and 20% silica by weight) with 55 wt. % JSC-1 subjected to vacuum processing .....	10
15.	Micrograph showing the surface of the as-cast sulfur - 65 wt. % JSC-1 sample .....	11
16.	Micrograph showing the surface of the sulfur - 65 wt. % JSC-1 sample after 8 days in vacuum .....	11
17.	Micrograph showing the surface of the sulfur - 65 wt. % JSC-1 sample after 58 days in vacuum .....	12

## LIST OF FIGURES (Continued)

18.	Micrograph showing the surface of the as-cast sulfur and silica binder mixture (25% sulfur and 20% silica by weight) with 55 wt. % JSC-1 sample .....	12
19.	Micrograph showing the surface of the silica binder mixture (25% sulfur and 20% silica by weight) with 55 wt. % JSC-1 sample after 8 days in vacuum .....	13
20.	Micrograph showing the surface of the silica binder mixture (25% sulfur and 20% silica by weight) with 55 wt. % JSC-1 sample after 58 days in vacuum .....	13
21.	Plot of the sulfur weight loss for the exposed surface area ( $\text{mg}/\text{mm}^2$ ) as a function of time .....	14
22.	Macrograph of the sulfur - 65 wt. % JSC-1 sample after 8 days in vacuum that represents the green diamond datum point, figure 21 .....	22
23.	Comparison of measured weight loss for pure sulfur with the Hertz-Knudsen equation, $\alpha_v = 1$ .....	16
24.	Comparison of the measured weight loss for pure sulfur and the sulfur concrete samples with the Hertz-Knudsen equation, $\alpha_v = 1$ , and with volume fraction, $v_f$ , correction factors .....	18
25.	Photograph of two samples exposed to vacuum for 60 days: left: sulfur - 35 wt. % JSC-1 and right: 25% sulfur and 20% silica by weight with 55 wt. % JSC-1 .....	19
26.	Calculated plot showing the effect of temperature on the time needed to sublimate a 1-cm (0.4-in) thickness of pure sulfur .....	19
27.	Calculated plot showing the role the ambient pressure plays in regard to the equilibrium vapor pressure .....	20
28.	Typical 2.54-cm (1-in) cube of sulfur concrete used in this study .....	22
29.	A typical time temperature plot showing one of the cycles the samples experienced .....	23
30.	Photograph of a sample undergoing compression testing at $-101\text{ }^\circ\text{C}$ ( $-150\text{ }^\circ\text{F}$ ) .....	24
31.	Photograph of cracking exhibited on the surface of sample 22, which was subjected to 80 cycles between RT ( $\approx 21\text{ }^\circ\text{C}$ , or $70\text{ }^\circ\text{F}$ ) and $-191\text{ }^\circ\text{C}$ ( $-312\text{ }^\circ\text{F}$ ). .....	24
32.	Plot of the maximum compression strength exhibited by the cycled and noncycled samples .....	25

## LIST OF FIGURES (Continued)

33.	SEM micrograph of a fracture surface from noncycled sample 10, a silica binder mixture (25% sulfur and 20% silica by weight) with 55 wt. % JSC-1, tested at 21 °C (70 °F) .....	26
34.	SEM micrograph of a fracture surface from noncycled sample 14, with the same composition as in figure 33, but tested at –101 °C (–150 °F) .....	26
35.	SEM micrograph of a fracture surface from cycled sample 22, a silica binder mixture (25% sulfur and 20% silica by weight) with 55 wt. % JSC-1, tested at 21 °C (70 °F) .....	27
36.	SEM micrograph of a fracture surface from cycled sample 24, with the same composition as in figure 35, but tested at –101 °C (–150 °F) .....	27
37.	SEM micrograph of a fracture surface from noncycled sample 4, a sulfur with 65 wt. % JSC-1 sample tested at 21 °C (70 °F) .....	28
38.	SEM micrograph of a fracture surface from noncycled sample 6 with the same composition as in figure 37, but tested at –101 °C (–150 °F) .....	29
39.	SEM micrograph of a fracture surface from cycled sample 18, a sulfur with 65 wt. % JSC-1 sample tested at 21 °C (70 °F) .....	29
40.	SEM micrograph of a fracture surface from cycled sample 20 with the same composition as figure 39, but tested at –101 °C (–150 °F) .....	30
41.	Photograph of a sulfur sample with 65 wt. % pure SiO <sub>2</sub> .....	32
42.	Photograph of a sample like that seen in figure 7 which was cycled 20 times between RT and –196 °C (–321 °F). Crumbling of the sample with free grains of silica is seen .....	32

## LIST OF ACRONYMS AND SYMBOLS

°C	degrees Celsius
°F	degrees Fahrenheit
°R	degrees Rankine
cm	centimeter
FeS	troilite, iron sulfide
g	gram
JSC-1	Johnson Space Center lunar soil simulant
K	Kelvin degree
LN <sub>2</sub>	liquid nitrogen
m	meter
mg	milligram
mm	millimeter
MPa	megapascal
Pa	Pascal
psi	pounds per square inch
S	sulfur
Sb	antimony
SEM	Scanning Electron Microscope
SiO <sub>2</sub>	silica, silicon dioxide
wt. %	percent by weight



## NOMENCLATURE

$L$	original length
$m$	atomic mass
$P$	ambient pressure
$P^*$	partial pressure of gas in equilibrium with its solid
$R$	gas constant
$RT$	room temperature
$T$	temperature
$vf$	volume fraction
$\alpha$	coefficient of thermal expansion
$\alpha_v$	evaporation coefficient
$\Gamma$	mass evaporation rate
$\Delta L$	change in original length
$\Delta T$	temperature difference
$\varepsilon$	strain



## TECHNICAL MEMORANDUM

### SULFUR ‘CONCRETE’ FOR LUNAR APPLICATIONS— ENVIRONMENTAL CONSIDERATIONS

#### 1. INTRODUCTION

Conventional concrete consists of sand, a coarser aggregate, and a hydraulic binder based on calcium silicate. Added water chemically reacts with the calcium silicate which then effectively sets up and hardens into the mass known as concrete. Sulfur ‘concrete’ is somewhat a misnomer, as very little, if any, chemical reaction occurs between the constituent materials. Basically the sulfur, a thermoplastic material, is melted and mixed with an aggregate, after which the mixture is poured, molded, and allowed to harden. As such, it is an established construction material<sup>1-17</sup> that has gained wide acceptance, particularly for use in environments subjected to acids and salts, figures 1-4.<sup>1</sup> It exhibits good compressive strength (generally better than Portland cement), low water permeability, and rapid setup times.



Figure 1. Eight-cubic-yard heater-mixer mobile production unit.

The composite composition generally ranges from 12–22 percent by weight, or weight percent (wt. %) sulfur and 78–88 wt. % aggregate, which can consist of any number of materials, including rock sands, minerals, fly ash, rubber particles, and glasses. The mixture can also contain some 5% of a group of compounds termed plasticizers that mitigate cracking as the sulfur goes through, at  $\approx 96\text{ }^{\circ}\text{C}$  ( $\approx 205\text{ }^{\circ}\text{F}$ ), a reversible monoclinic-rhombic crystalline phase change. One downside is sulfur’s narrow working range. It melts at  $\approx 120\text{ }^{\circ}\text{C}$  ( $248\text{ }^{\circ}\text{F}$ ), but above  $148\text{ }^{\circ}\text{C}$  ( $298\text{ }^{\circ}\text{F}$ ) the liquid experiences a phase change where it ‘stiffens’ and loses needed fluidity. Making and applying sulfur concrete is generally constrained between  $130$  and  $140\text{ }^{\circ}\text{C}$  ( $266$  and  $284\text{ }^{\circ}\text{F}$ ) and, obviously, it cannot be used in an environment that exceeds  $\approx 120\text{ }^{\circ}\text{C}$  ( $248\text{ }^{\circ}\text{F}$ ).



Figure 2. Pouring of Chempruf Sulfur Concrete in an industrial plant.



Figure 3. Chempruf Sulfur Concrete: acid containment system.



Figure 4. Precast Chempruf Sulfur Concrete tanks for Aqua Regia.

Sulfur has been found on the Moon in the form of the mineral troilite,  $\text{FeS}$ ,<sup>18,19</sup> which raises the question of reducing the ore to obtain sulfur for construction purposes. This is an attractive alternative to conventional concrete, as water, a precious resource, is not required. Reducing troilite to elemental

sulfur and using sulfur concrete on the Moon has been previously discussed.<sup>20-27</sup> For our purposes it is assumed that elemental sulfur is available on the lunar surface and sulfur concrete products such as bricks can be made.

Acknowledging that environmental conditions on Earth are relevant to the use of sulfur concrete, it follows that lunar applications would entail additional concerns. Lunar temperatures at the equator range from +123 to -180 °C (253 to -292 °F), with an average of -20°C (-4 °F) and, at the poles, from -60 to -220 °C (-76 to -364 °F). These are extreme temperatures and, perhaps more important, extreme temperature cycles. How this might affect the mechanical properties of sulfur concrete is unknown. Secondly, the Moon's environment is also characterized by a lack of atmosphere, generally assumed to be on the order of  $1 \times 10^{-12}$  torr ( $1.33 \times 10^{-10}$  Pa). This low pressure brings into question sublimation processes where a material that is a stable solid at 1 atmosphere (atm) would now transform to a gaseous state.

Clearly it can be expected that these extremes in temperature and pressure will affect the viability of sulfur concrete. The following sections will evaluate, as best as possible, these environmental concerns, with the intent of ascertaining the feasibility of using sulfur concrete as a construction material on the lunar surface.

## 2. SUBLIMATION CONSIDERATIONS

A well known example of sublimation on Earth is where solid carbon dioxide (dry ice), upon warming, directly transforms to gas. Some insight to sulfur sublimation can be gained by examination of its unary pressure-temperature phase diagram.<sup>28</sup> Note that this phase diagram is not particularly well understood and several generally similar versions, such as the one seen in figure 5, can be found.

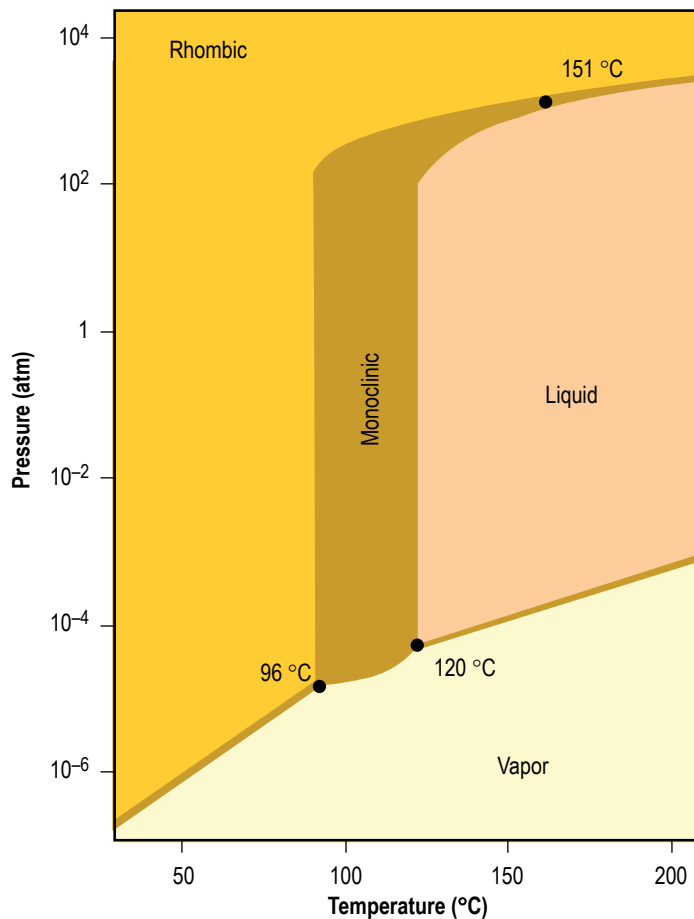


Figure 5. Typical unary sulfur phase diagram.

Given that, on Earth at 760 torr (1 atmosphere, 0.1 MPa), as the temperature rises from room temperature ( $\approx 20$  °C (68 °F)), sulfur undergoes a solid phase transition—here  $\approx 96$  °C (205 °F)—and then melts at  $\approx 120$  °C ( $\approx 248$  °F). In contrast, at pressures on the order of  $7.6 \times 10^{-3}$  torr (1.0132 Pa), solid sulfur transforms directly, or sublimates, to a gaseous phase at  $\approx 90$  °C (194 °F); the transition temperature continues to decrease with decreasing pressure.<sup>28, 29</sup> Recall the pressure on the Moon,  $\approx 1 \times 10^{-12}$  torr ( $1.33 \times 10^{-10}$  Pa), and it is realistic to assume that the sulfur composing sulfur concrete

would be prone to sublime, resulting in a deteriorated, unsound, structure. With that in mind, the intent of this work is to study the effect of a high and prolonged vacuum on pure sulfur and two presumed lunar-like sulfur ‘concrete’ compositions.

## 2.1 Experimental Procedure

Pure sulfur and sulfur ‘concrete’ mixtures of two different compositions were prepared for evaluation. The pure sulfur was melted and cast into small, circular, hard plastic molds  $\approx 45$  mm (1.8 in) in diameter and 5 mm (0.2 in) deep. The approximate compositions of the concrete samples were: (1) 35 wt. % pure sulfur with 65 wt. % JSC-1 (an established lunar simulant soil<sup>30</sup> that has a sand-like consistency) and (2) a sulfur and silica binder mixture (25% sulfur and 20% silica by weight) with 55 wt. % JSC-1. The sulfur-silica binder is a commercially available product known as Gilson Rediron 9000 Capping Compound, American Society for Testing Materials (ASTM) C617 and American Association of State Highway and Transportation Officials (AASHTO) T231. The sulfur, or binder mixture, is melted and mixed with the aggregate which is then poured into heated molds having dimensions of  $2 \times 2 \times 2$  in ( $\approx 50$  mm each side) with excess added to account for shrinkage. The cube is allowed to cool, after which it is removed and readied for testing, a procedure that generally entails sectioning the block into pieces such as seen in figure 6. Additional experimental details can be found elsewhere.<sup>25–27</sup>



Figure 6. A piece of sulfur-based concrete made at The University of Alabama in Huntsville. The corners were broken off for testing purposes.

The sublimation experiments were conducted in a vacuum chamber, figure 7, which is capable of achieving a vacuum level on the order of  $5 \times 10^7$  torr ( $6.67 \times 10^5$  Pa), a level below which sublimation of sulfur at 20 °C (68 °F) is expected upon extrapolation of the pressure/temperature lines shown in figure 8, another variation of the unary sulfur pressure-temperature diagram. Here the green square marks the prescribed experimental conditions and suggests that sublimation of the sulfur from the concrete composite will occur.



Figure 7. Photograph of the vacuum chamber used for the sublimation experiments.

To verify that sublimation under the proposed experimental conditions—room temperature (RT) and  $6.67 \times 10^{-5}$  Pa—would actually occur, one of the broken-off corners of the sample shown in figure 6 was placed in the chamber. After approximately 6 days at  $\approx 3 \times 10^{-6}$  torr and  $\approx 20$  °C ( $\approx 68$  °F), the sample was removed for examination. Figure 9 shows the piece subjected to vacuum processing, in the upper right hand corner, matched with the untested section from which it was broken. The surface of the processed sample exhibits obvious porosity enhancement and a granular morphology. It is further noted that the initial piece weighed 2.1449 g (0.0047 lb) and after removal weighed 2.0416 g (0.0045 lb), essentially losing  $\approx 0.1$ g (0.0002 lb) of sulfur. The loss is not likely due to water vapor or other volatiles, as the sample was placed in an oven overnight at 110 °C (230 °F) prior to its being weighed and placed in the vacuum chamber.

For the controlled sublimation study, small sections on the order of 10 mm  $\times$  5 mm  $\times$  3 mm (0.393  $\times$  0.196  $\times$  0.116 in) were cut from a cube representative of the two concrete compositions and weighed. One piece of each composition was placed, large surface area down, in a small aluminum weighing dish; six sets were prepared. The six sample sets were then placed in the chamber and subjected to vacuum processing. Every 5 to 10 days, the chamber was opened and the samples removed for weighing; one composition set was kept out and the remaining were put back in the vacuum chamber. Generally speaking, a vacuum level on the order of  $3\text{--}7 \times 10^{-6}$  torr ( $4\text{--}9.3 \times 10^{-4}$  Pa) was observed during processing. The samples removed during testing were weighed and their surfaces photographed. The exposed surface area of each sample was measured and the recorded weight loss from sublimated sulfur was expressed as milligrams per square millimeter ( $\text{mg}/\text{mm}^2$ ). This scenario was kept up, more or less, for 60 days. A similar scenario was independently conducted for the pure sulfur samples. The pure sulfur samples were kept in the plastic molds described above, their surfaces left to be exposed to the vacuum.

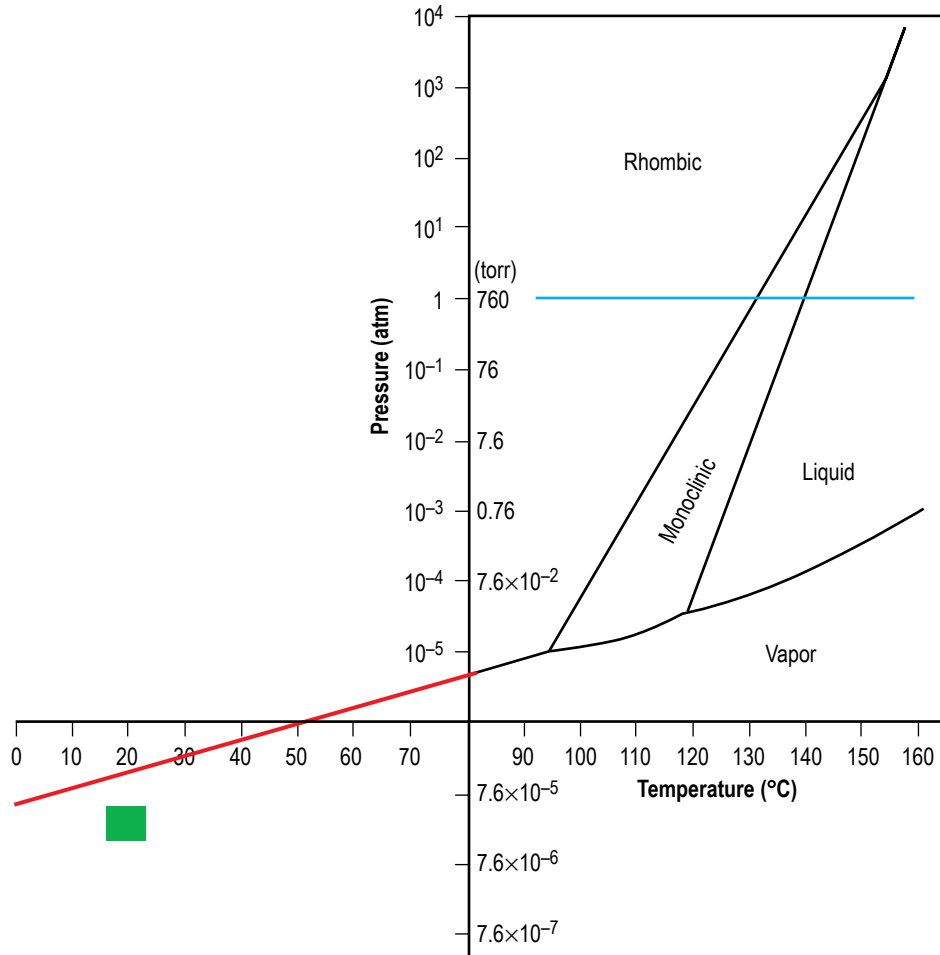


Figure 8. Extrapolation of the solid-vapor transition line on a unary sulfur phase diagram.

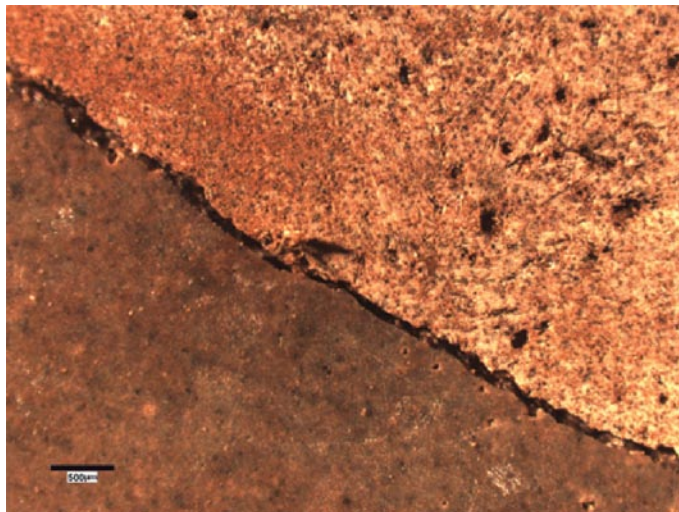


Figure 9. Comparison of the sulfur concrete surfaces after vacuum processing of the upper right-hand corner section.

## 2.2 Experimental Results

Figures 10–12 show representative surfaces of the as-cast pure sulfur and samples that have been exposed to vacuum. First of all, the surface of an ‘as-cast’ sample, figure 10, is not smooth or uniform, the obvious irregularities being shrinkage effects such as cavities and dendrite in-filling with a glazed appearance. After 11 days in vacuum, as shown in figure 11, sulfur sublimation clearly reveals the intricate nature of the primary dendrites. Figure 12 shows a typical surface after 54 days in vacuum. Here the shrinkage cavities have grown and the fibrous nature of the dendritic crystals is accentuated.

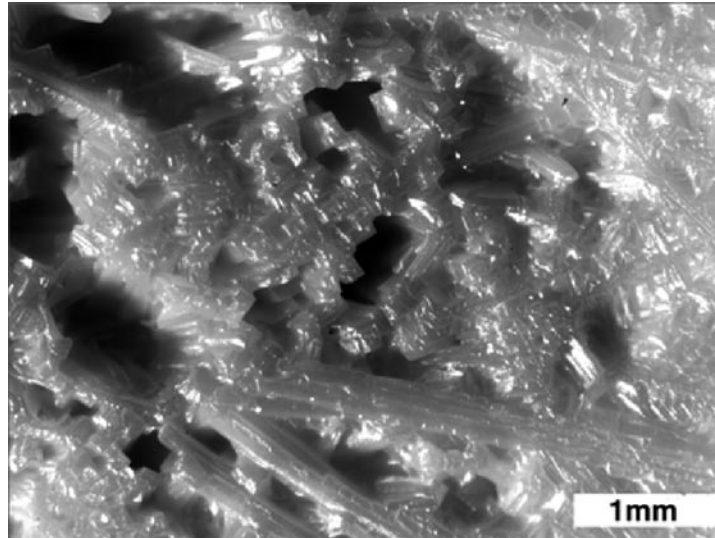


Figure 10. Surface morphology of the as-cast pure sulfur.

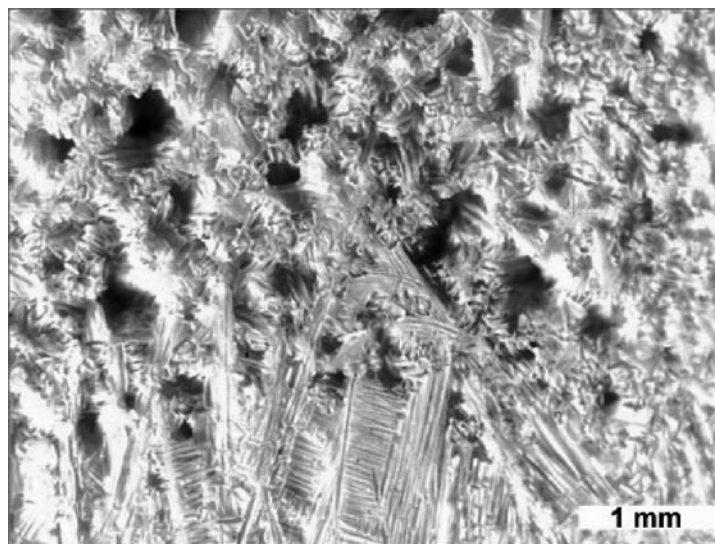


Figure 11. Surface morphology of the as-cast pure sulfur after vacuum processing on the order of  $3\text{--}7 \times 10^{-6}$  torr ( $4\text{--}9.3 \times 10^{-4}$  Pa) for  $\approx 11$  days.

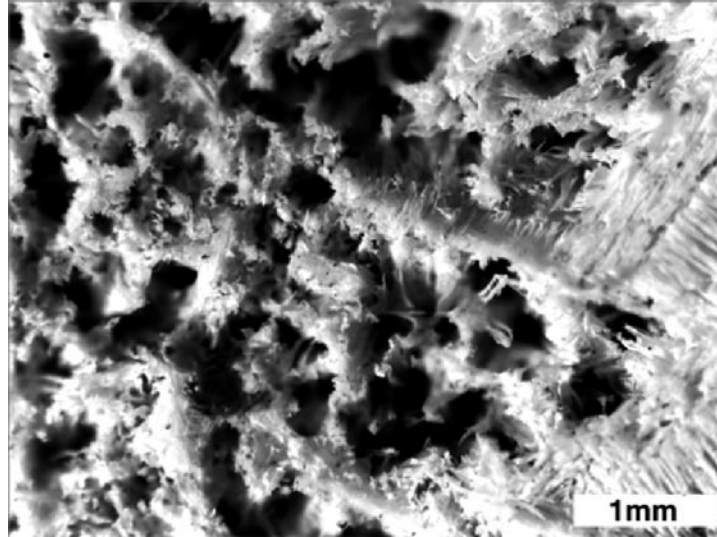


Figure 12. Surface morphology of the as-cast pure sulfur after vacuum processing on the order of  $3-7 \times 10^{-6}$  torr ( $4-9.3 \times 10^{-4}$  Pa) for  $\approx 54$  days.

Figures 13 and 14 show, respectively, the surfaces of the samples removed from vacuum after 8, 15, 25, 39, 46, and 58 days. Samples in figure 13 have the sulfur - 65 wt. % JSC-1 (Johnson Space Center lunar soil simulant) composition, and those in figure 14 consist of the sulfur and silica binder mixture

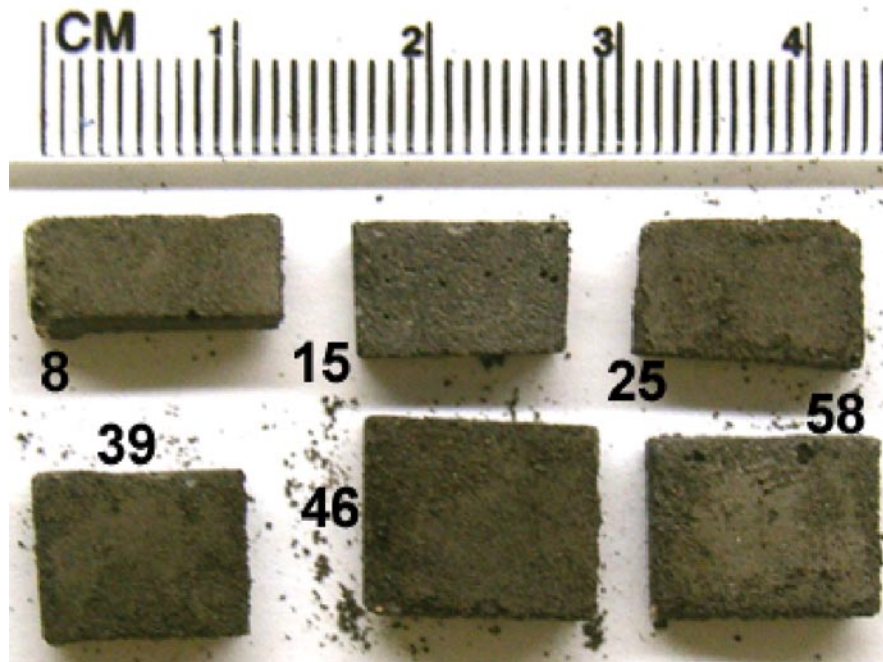


Figure 13. Sulfur - 65 wt. % JSC-1 samples subjected to vacuum processing. Numbers indicate days processed.

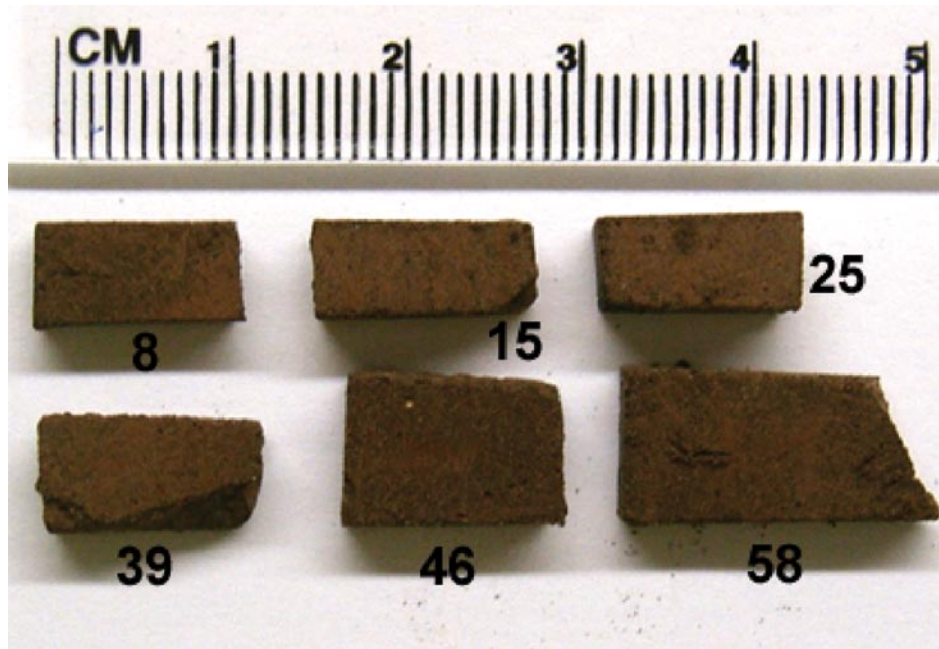


Figure 14. Sulfur and silica binder mixture (25% sulfur and 20% silica by weight) with 55 wt. % JSC-1 subjected to vacuum processing. Numbers indicate days processed.

(25% sulfur and 20% silica by weight) with 55 wt. % JSC-1. Obvious and increasing degradation of the samples as a function of time is seen, particularly in figure 13, whose samples have 10% more sulfur than those in figure 14.

Figures 15–20 are representative micrographs of sample sulfur ‘concrete’ surfaces shown above. Figure 15 shows the surface of the as-cast, sulfur - 65 wt. % JSC-1, sample, figure 16 shows that sample after 8 days’ exposure to vacuum, and figure 17 after 58 days. Figures 18–20 are similar except that the samples contain  $\text{SiO}_2$  and less sulfur. The as-cast surfaces are relatively smooth; clear degradation of the surface is seen after 8 days, more so after 58 days. Again, the extent of degradation is obviously more apparent in figures 17 and 18, showing the concrete samples containing the greatest amount of sulfur.

Figure 21 plots the measured sulfur weight loss, normalized to milligram per square millimeter ( $\text{mg}/\text{mm}^2$ ) of exposed surface area, as a function of time. As seen, the number of points for a given composition decreases with time due to the removal of one sample at each examination period to assess surface degradation. Although scatter within the individual samples is seen, clear trends for the given sample compositions are apparent. The graph shows, as figures 10–12 and 15–20 suggest, the greater the amount of initial sulfur in the sample, the more that will sublime away over a given period. The rate of sublimation also decreases with time, and one might also infer, particularly for the aggregate containing samples, that they will reach some constant value.

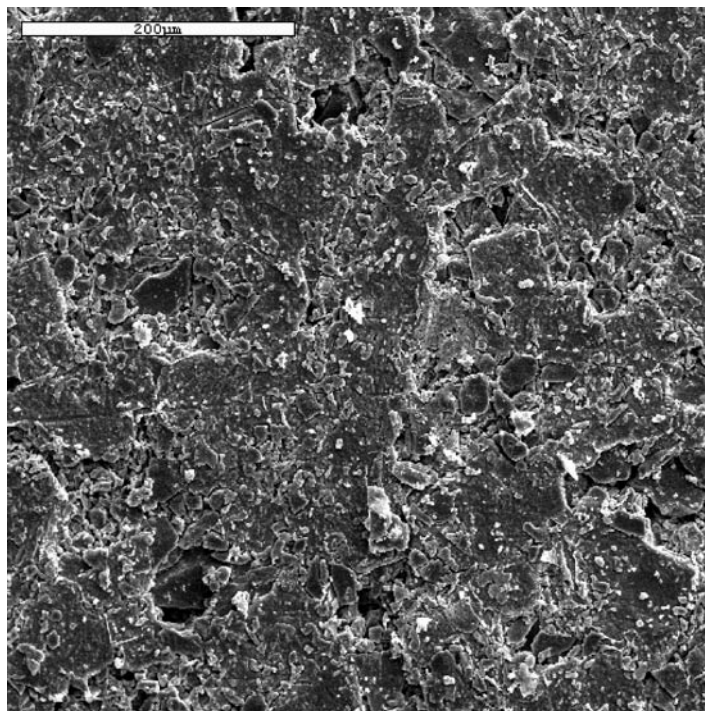


Figure 15. Micrograph showing the surface of the as-cast sulfur - 65 wt. % JSC-1 sample.

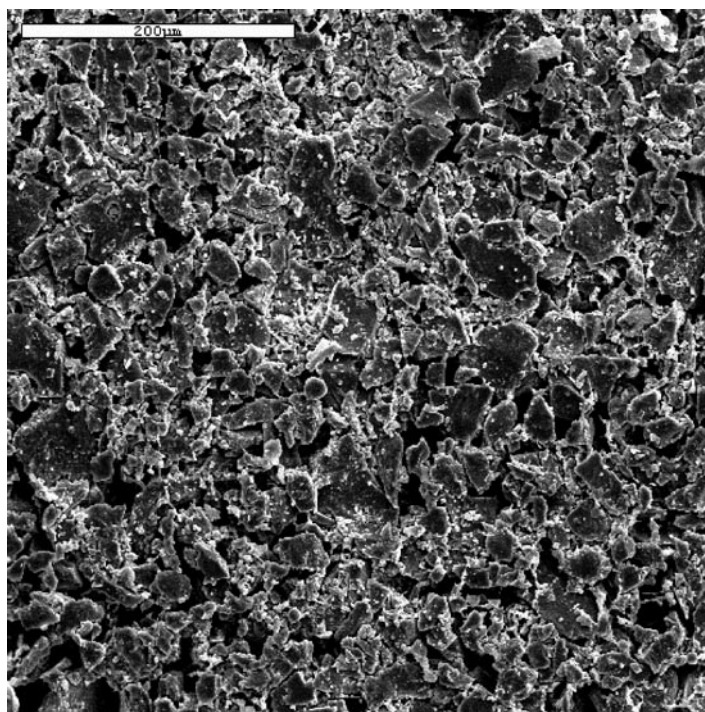


Figure 16. Micrograph showing the surface of the sulfur - 65 wt. % JSC-1 sample after 8 days in vacuum.

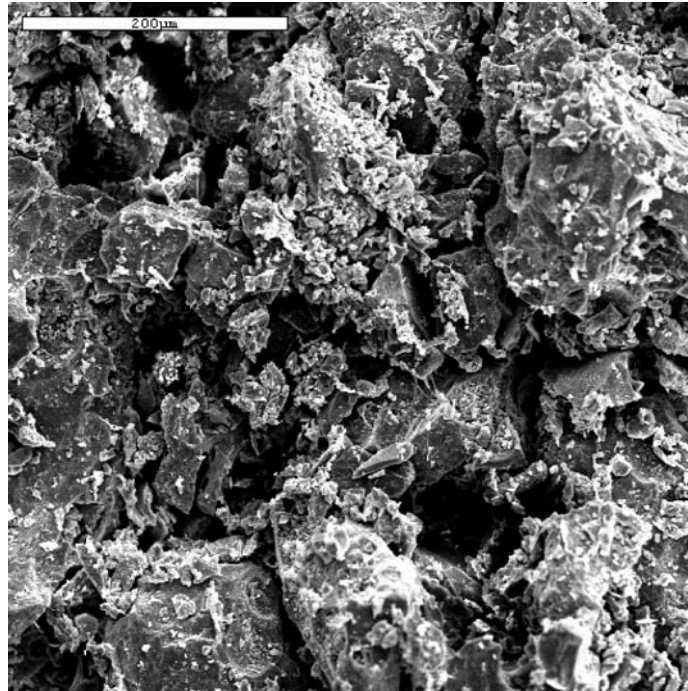


Figure 17. Micrograph showing the surface of the sulfur - 65 wt. % JSC-1 sample after 58 days in vacuum.

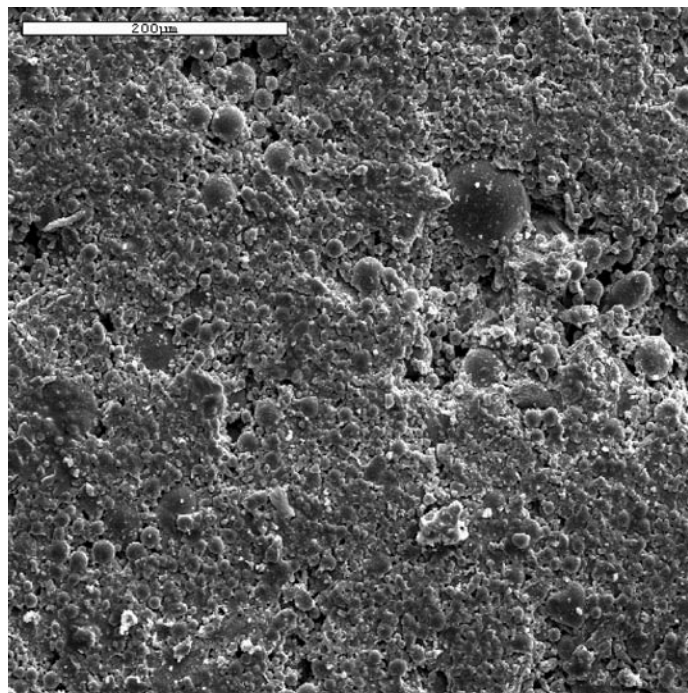


Figure 18. Micrograph showing the surface of the as-cast sulfur and silica binder mixture (25% sulfur and 20% silica by weight) with 55 wt. % JSC-1 sample.

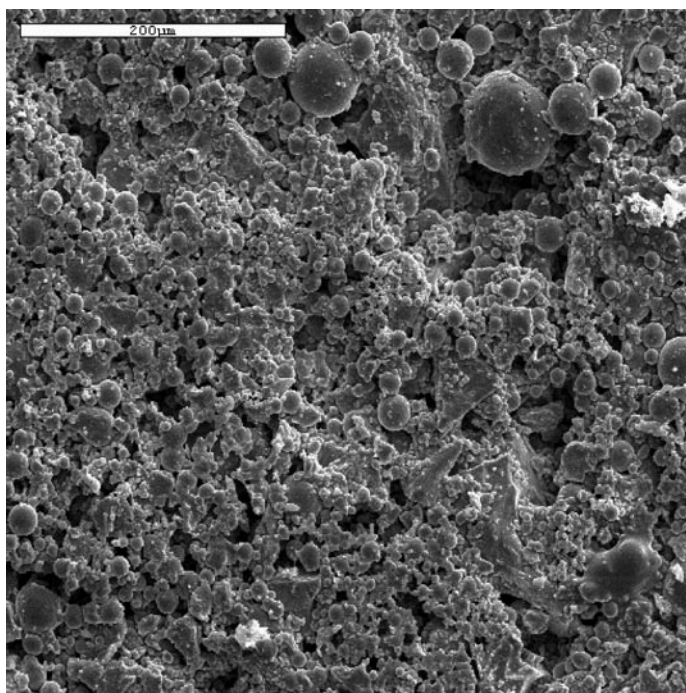


Figure 19. Micrograph showing the surface of the silica binder mixture (25% sulfur and 20% silica by weight) with 55 wt. % JSC-1 sample after 8 days in vacuum. The spherical particles are the SiO<sub>2</sub> grains.

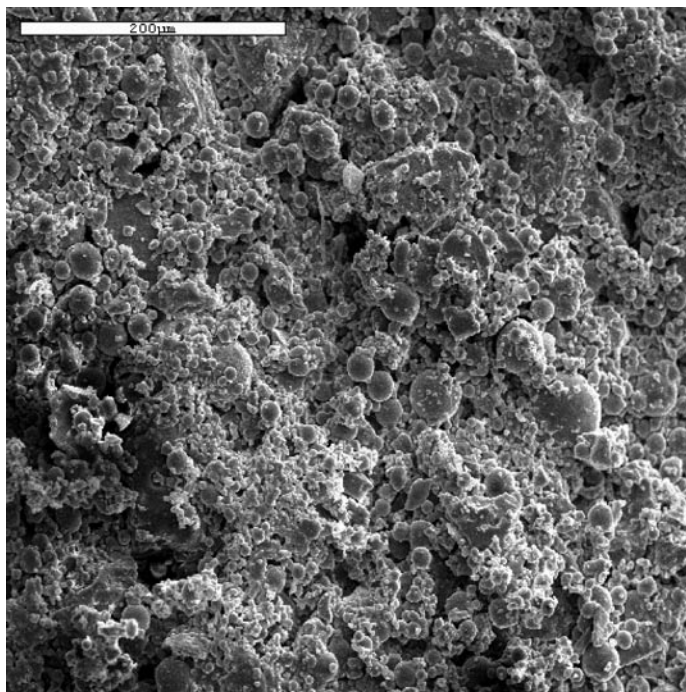


Figure 20. Micrograph showing the surface of the silica binder mixture (25% sulfur and 20% silica by weight) with 55 wt. % JSC-1 sample after 58 days in vacuum.

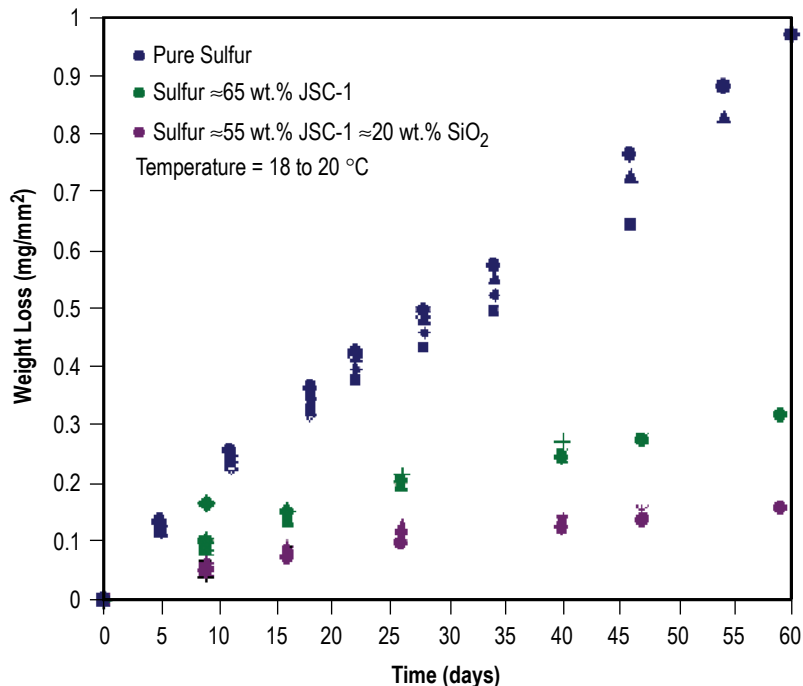


Figure 21. Plot of the sulfur weight loss for the exposed surface area ( $\text{mg}/\text{mm}^2$ ) as a function of time.

### 2.3 Discussion of Sublimation Concerns

Figure 21 shows clear trends in sulfur sublimation as a function of sample material. Still, there is obvious scatter in the weight loss/surface area for a given set of samples. This is attributed to several factors. For instance, the actual surface area measurement of the sample is probably off by  $\pm 5\%$ . In addition, the surface area measurement is strictly a bulk sample consideration. Examination of figures 10, 15, and 18 clearly shows that the stated surface area does not consider surface irregularities such as ledges and porosity. After vacuum processing, the sublimated voids further add to the surface area. Additional scatter in the data could arise from nonuniform distribution of aggregate; more at the surface on a given sample would show less weight loss. It is also assumed that the sublimation rate is uniform on the sample surface and sides; the bottom area in contact with the aluminum pan is ignored. Some insight to this latter assumption was inadvertently obtained. In figure 21 the green diamond datum point representing the sulfur - 65 wt. % JSC-1 sample after 8 days is uncharacteristically high. Examination of the sample showed that after cutting the sample from the bulk, a small ‘leg’ was unintentionally left on the sample,<sup>26</sup> as shown in figure 22.

This effectively raised the sample bottom from the aluminum pan and exposed additional area from which sulfur could easily sublimate. One must also consider that over time, as the sulfur sublimates away, more and more of the aggregate is exposed. In this case, any now ‘free’ aggregate would sit on the sample surface, effectively blocking any sulfur underneath from leaving. If this same piece is placed on its side, its large surface area now parallel to a gravity vector, exposed aggregate may well fall off, exposing fresh sulfur for sublimation. In summary, scatter in the observed data should be expected and is dependent on, at least, aggregate size, shape, distribution, and sample exposure position.



Figure 22. Macrograph of the sulfur - 65 wt. % JSC-1 sample after 8 days in vacuum that represents the green diamond datum point, figure 21. The ‘leg’ inadvertently left on the sample effectively exposed more surface area and resulted in a greater mass of lost sulfur.

Consider now the sublimation data for the individual sample compositions: (1) pure sulfur, (2) sulfur with 65 wt. % JSC-1, and (3) the sulfur-silica binder and 55 wt. % JSC-1 mixture. Obviously, as seen, the sample with the most sulfur per unit bulk surface area will sublimate away the most. Given that, weight loss per surface area for pure sulfur appears nearly constant with time, whereas the other two compositions give the impression of decreasing slightly with time. The evaporation rate of sulfur can be evaluated using the well known Hertz-Knudsen equation<sup>31-33</sup> given below.

$$\Gamma = \alpha_v \left( \frac{m}{2\pi RT} \right)^{1/2} (P^* - P) . \quad (1)$$

Here  $\Gamma$  is the mass evaporation rate,  $\alpha_v$  is designated as an evaporation coefficient,  $m$  is the atomic mass (32.06 for sulfur),  $R$  is the gas constant ( $8.31432 \text{ J}\cdot\text{K}^{-1}\cdot\text{mol}^{-1}$ ),  $T$  is the absolute temperature (293 K for this work),  $P^*$  is the partial pressure of the gas phase in equilibrium with its solid (assumed to be  $1.8 \times 10^{-6}$  torr or  $2.4 \times 10^{-4}$  Pa), and  $P$  is the ambient (obtainable) pressure of the experimental vacuum chamber ( $5 \times 10^{-7}$  torr or  $6.67 \times 10^{-5}$  Pa). The evaporation coefficient,  $\alpha_v$ , was introduced and justified by Knudsen as a consequence of experimental results being less than that predicted by equation (1) in its basic form. Also known as a ‘sticking’ coefficient,  $\alpha_v$  is a measure of the difficulty for atoms to either attach to or be released from a surface, and ascertaining its value is fraught with difficulty.<sup>34</sup> Values of  $\alpha_v \approx 1$  were reported for tungsten,<sup>35</sup> copper and iron,<sup>36</sup> nickel and nickel oxide,<sup>37</sup> and beryllium.<sup>38</sup> Other values for  $\alpha_v$  include 0.17 for Sb at 650 K (1,170 °R),<sup>39</sup> 0.17 for LiF at 1,000 K (1,800 °R),<sup>40</sup> and 0.1–0.4 for the KCl-NaCl system between 913 K (1,643 °R) and 1,033 K (1,859 °R).<sup>41</sup> A value of  $4.6 \times 10^{-3}$  was also measured for arsenic at 550 K (990 °R).<sup>42</sup> No value of  $\alpha_v$  for sulfur could be found, so it was, for purposes of calculation, assumed to equal 1.

Using the above values, evaluation of equation (1) results in an evaporation rate for pure sulfur of  $\Gamma = 2.50808 \times 10^{-8} \text{ g}\cdot\text{cm}^{-2}\cdot\text{s}^{-1}$  ( $2.50808 \times 10^{-7} \text{ mg}\cdot\text{mm}^{-2}\cdot\text{s}^{-1}$ ); this ideally translates, at 20 °C (68 °F), to sublimating away a 1-cm-thick (0.4-in-thick) layer of sulfur in  $\approx 955$  days. Consequently, assuming a uniform sample surface area of 962.1 mm<sup>2</sup>, one might expect to lose  $\approx 2.413 \times 10^{-4} \text{ mg/s}$  of sulfur from the sample. If this value remained constant for the length of the experiment (60 days at 18–20 °C, or 64–68 °F), 1.251 g of sulfur would sublimate. Experimentally, the pure sulfur sample that was exposed to vacuum for 60 days lost 0.9329 g.

The Hertz-Knudsen equation for pure sulfur and the experimental conditions are plotted in figure 23. Examination reveals good agreement, assuming  $\alpha_v = 1$ , for the first 10 days or so, after which increasing deviation is seen.

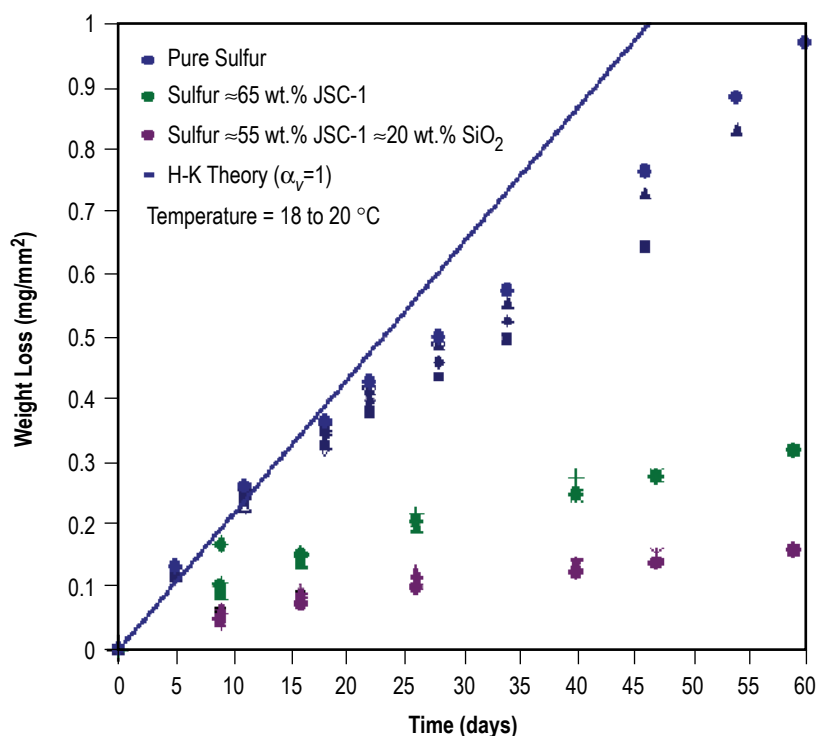


Figure 23. Comparison of measured weight loss for pure sulfur with the Hertz-Knudsen equation,  $\alpha_v = 1$ .

The higher initial rate of sulfur sublimation can be inferred from figures 10–12. This as-cast material has the greatest surface area, as shown in figure 10, from which to draw atoms. The surface is essentially composed of a dendritic network, the arms in-filled with the last material to solidify, giving it a glazed appearance. This in-filled surface material would contain the majority of any impurities, have a slightly lower melting temperature, and possibly have greater volatility. This postulate is supported by figure 11, which shows emergence and clear definition of the primary (highest melting point) dendritic structure. The surface seen in figure 11 has also been subjected to vacuum for 11 days, approximately the time at which the sublimation rate is seen to begin decreasing, (see fig. 23). This decrease in

sublimation rate can be attributed to at least two factors. First, the cavities would still contain the residual solidification product, but their deepening now increases the difficulty for sulfur atoms to leave. Second, the surface now consists of well exposed, but randomly oriented, dendrites that grow in specific crystallographic directions. The exposed dendrite arms constitute a mesh that could obstruct released atoms, and it is further expected that the release rate of atoms will differ (e.g., Inaba<sup>43</sup>) for each crystallographic orientation. Thus it is prudent to note that the assumption of  $\alpha_v = 1$  may have been fortuitous and that an appropriate evaluation of its true value would entail specifically designed equipment in conjunction with a sulfur single crystal of known orientation. Finally, figure 12 (54 days in vacuum) shows increasing size of the shrinkage cavities and further detail of the dendrite structure; the evaporation rate continues to slowly decrease.

Obviously, as the aggregate mixtures contained less sulfur, sublimation rates were expectedly less for them, figures 16–20. The densities ( $\rho$ ) of sulfur and  $\text{SiO}_2$  are,<sup>44</sup> respectively,  $2.07 \text{ g cm}^{-3}$  and  $2.32 \text{ g cm}^{-3}$ ; the density<sup>30</sup> of JSC-1 is  $2.9 \text{ g cm}^{-3}$ . Converting the sulfur  $\approx 65$  wt. % JSC-1 composition and 25% sulfur and 20% silica by weight with 55 wt. % JSC-1 composition samples to volume percentages finds the former to be 57.0 volume percent aggregate (43% S) and the latter to be 69.55 volume percent aggregate (30.45% S). To a first approximation, reasonably noting that the aggregate material does not sublime, volume fraction factors,  $v_f$  (0.43 and 0.3) can be placed in conjunction with the evaporation coefficient; the Hertz-Knudsen equation with this correction factor included is plotted for the two mixtures in figure 24.

Again, early fit with the data is seen, but the theory soon over-predicts the experimental results. This is expected, particularly in view of figures 15–20. Initially the sample surfaces are relatively smooth with little, if any, of the aggregate exposed. More and more of the aggregate is exposed as sublimation proceeds. This effectively reduces the amount of exposed sulfur, assuming the aggregate does not fall away, which over time leaves less to sublime through an increasingly difficult path. Figure 25 shows the surface of two samples that were exposed to vacuum for 60 days. On the left is the sulfur - 65 wt. % JSC-1 sample and on the right is sulfur  $\approx 55$  wt. % JSC-1  $\approx 20$  wt. %  $\text{SiO}_2$ . The surface discoloration is a consequence of mechanically removing the vacuum affected material. Although the sulfur sublimed, the aggregate particles remained cohesively in place, e.g. figures 13 and 14. However, they could be easily removed by a disturbance as mild as gentle tapping.

The vacuum-exposed surface of the sulfur - 65 wt. % JSC-1 sample (left, in fig. 25) is the reddish-brown triangular shape located at the central right. The darker brown region surrounding it is the material underneath and was easily exposed by a small air jet. The lighter stripe along the left side denotes the region where the brown material was gently scraped away, exposing hard and intact material. The exposed surface of the sulfur  $\approx 55$  wt. % JSC-1  $\approx 20$  wt. %  $\text{SiO}_2$  sample (fig. 25, right) is the wider strip of brownish-orange on the right side. The lighter strip on the left is where the loosely cohesive material was gently scraped away. The surface area of the samples is approximately  $6 \text{ mm} \times 11 \text{ mm}$ . Over a period of 60 days, see figure 24, the samples should have, left and right, lost 0.02178 and 0.01056 g of sulfur. For a surface area of  $66 \text{ mm}^2$ , these values translate to sulfur thicknesses of 0.159 mm and 0.0773 mm. Recall that the sulfur only accounts for  $\approx 43.0$  and  $\approx 30.45$  volume percent in these samples. When the aggregate is included, the overall volume fractions of the affected sample material are, respectively,  $24.47 \text{ mm}^3$  and  $16.75 \text{ mm}^3$ . This translates to thicknesses of 0.37 mm and 0.254 mm. In summary, the calculated thicknesses of the vacuum-affected zones are reasonably representative of

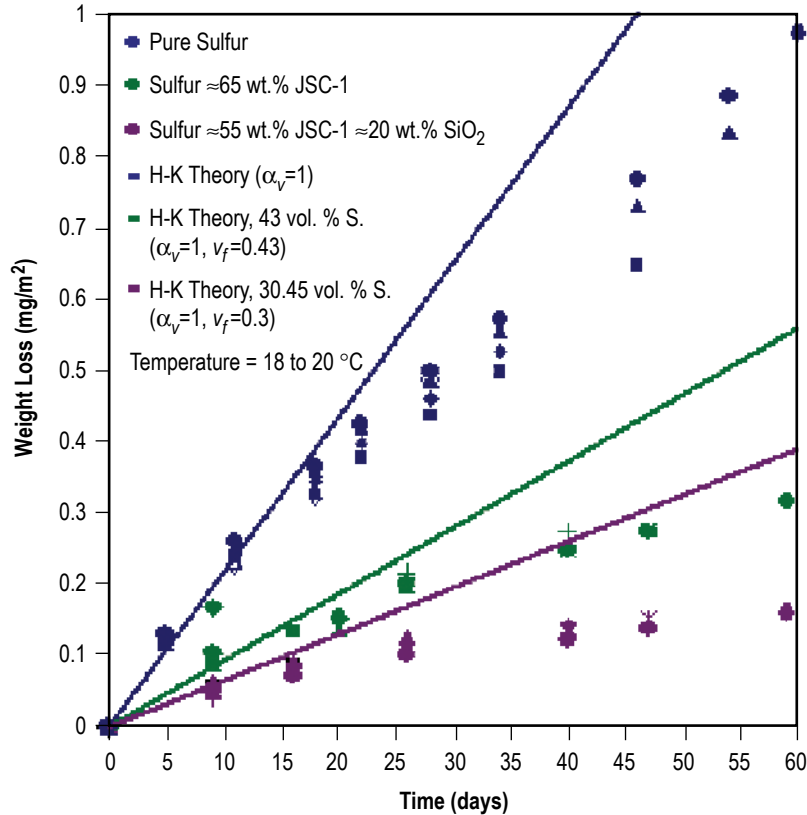


Figure 24. Comparison of the measured weight loss for pure sulfur and the sulfur concrete samples with the Hertz-Knudsen equation,  $\alpha_v = 1$ , and with volume fraction,  $v_f$  correction factors.

what was experimentally seen. What has been verified, at least for these samples and conditions, is that the affected depth is a function of the aggregate volume fraction. Put another way, assuming that the sulfur loss rate for the concrete samples becomes constant as suggested by figure 6, it would take  $\approx 4.4$  yr to sublimate to a depth of 1 cm in a sulfur  $\approx 65$  wt. % JSC-1 brick versus  $\approx 6.5$  yr for the sulfur  $\approx 55$  wt. % JSC-1  $\approx 20$  wt. %  $\text{SiO}_2$  composition. This, again, is drawn from data where the bulk of the exposed aggregate remained on the sample surface.

The experimental results and analysis presented above were confined to room temperature, i.e.,  $\approx 20^\circ\text{C}$  ( $68^\circ\text{F}$ ). Lunar temperatures vary considerably from this ( $-230$  to  $130^\circ\text{C}$ , or  $-382$  to  $266^\circ\text{F}$ ) and can significantly affect sublimation rates. Utilizing the Hertz-Knudsen equation in conjunction with the vapor pressure versus temperature curve,<sup>29</sup> the calculated curves shown in figure 26 plot the time to sublimate away a 1-cm-thick sulfur layer. Two pressures (Moon and experimental chamber) are considered between temperatures ranging from  $15$  to  $120^\circ\text{C}$  ( $59$  to  $248^\circ\text{F}$ ), the latter being near sulfur's melting point. At  $\approx 15^\circ\text{C}$  ( $\approx 59^\circ\text{F}$ ), the effect of a much lower lunar pressure is seen and a 1-cm (0.4-in) layer is calculated to take 3.7 yr to evaporate in comparison to 8.4 yr, which is calculated for the ground-based experimental chamber. Above  $\approx 30^\circ\text{C}$  ( $86^\circ\text{F}$ ), the two curves are essentially indistinguishable. However, the consequence of increasing temperature becomes obvious. What might be tolerable at  $15^\circ\text{C}$



Figure 25. Photograph of two samples exposed to vacuum for 60 days: left: sulfur - 35 wt. % JSC-1 and right: 25% sulfur and 20% silica by weight with 55 wt. % JSC-1.

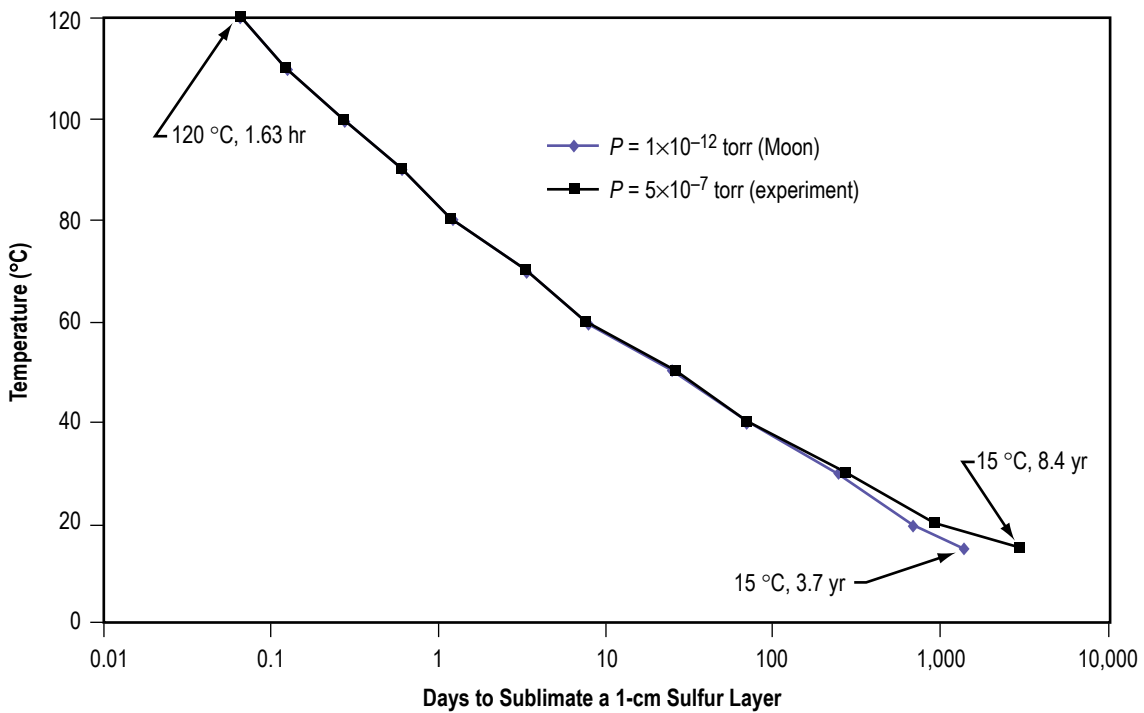


Figure 26. Calculated plot showing the effect of temperature on the time needed to sublimate a 1-cm (0.4-in) thickness of pure sulfur.

(59°F) is clearly not at  $\approx 120\text{ }^{\circ}\text{C}$  (248 °F), where it is calculated to take less than 2 hr to sublimate a 1-cm (0.4-in) layer.

The above work considers vacuum effects over time on pure sulfur and two sulfur concrete compositions at a temperature of  $\approx 20\text{ }^{\circ}\text{C}$  (68 °F). Other temperatures, or even cycles, can easily be implemented on the system to mimic lunar conditions and ascertain evaporation rates. What is difficult to reproduce is the lunar pressure, which is on the order of  $10^{-12}$  torr ( $1 \times 10^{-10}$  Pa). This raises the question of whether or not the results presented here, for the given temperature, are applicable to a lunar environment. Recall that the partial pressure of sulfur ( $P^*$ ) in equilibrium with its solid (at  $20\text{ }^{\circ}\text{C}$ , or 68 °F) was assumed to be  $1.8 \times 10^{-6}$  torr ( $2.4 \times 10^{-4}$  Pa) and that the vacuum chamber was able to reach an ambient level ( $P$ ) of  $\approx 5 \times 10^{-7}$  torr ( $6.67 \times 10^{-5}$  Pa). For a constant  $P^*$  and  $T$  the evaporation rate ( $\Gamma$ ), equation (1), should increase as  $P$  decreases. Thus, is it reasonable to assume that a laboratory chamber capable of  $5 \times 10^{-7}$  torr is representative of the lunar environment, which is smaller by some 5 orders of magnitude? The calculated results shown in figure 27 gauge the role vacuum level plays on the sublimation rate by plotting ( $P^*-P$ ) as a function of the environmental (ambient) pressure. At  $P = 1.8 \times 10^{-6}$  torr, ( $P^*-P$ ) is zero, but as  $P$  decreases, the designated degree of sublimation rapidly increases, being upper bound by a maximum of  $1.8 \times 10^{-6}$  when  $P$  equals zero. For an environmental pressure of  $5 \times 10^{-7}$  torr, this corresponds to a ( $P^*-P$ ) value that is 72.2% of the value achievable. Decreasing the pressure to  $1 \times 10^{-7}$  torr accounts for 94.4% and  $1 \times 10^{-8}$  torr relates to 99.4%. While it might be prudent to increase the measured sublimation rates by  $\approx 28\%$ , it is apparent that the much lower lunar atmosphere of  $10^{-12}$  torr would contribute only negligibly.

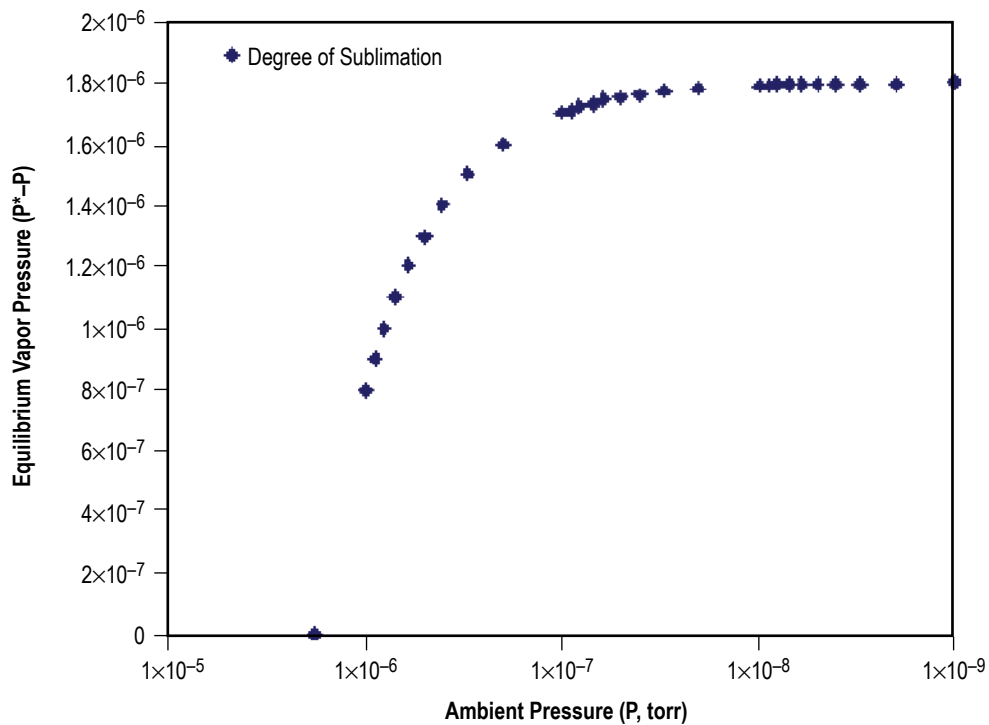


Figure 27. Calculated plot showing the role the ambient pressure plays in regard to the equilibrium vapor pressure.

## 2.4 Summary of Sublimation Concerns

Pure sulfur and two sulfur concrete mixtures were prepared and placed in a vacuum environment (capable of  $5 \times 10^{-7}$  torr) at  $\approx 20$  °C (68 °F) for 60 days. Periodic weighing of the samples revealed a continuous weight loss caused by the sublimation of sulfur. The sublimation rate was evaluated with the Hertz-Knudsen equation, assuming an evaporation coefficient of 1.0. Reasonable agreement over  $\approx 10$  days was found for pure sulfur and for the concrete mixtures when the volume fraction of added aggregate was considered. Subsequent discrepancies were attributed to nonuniform surfaces, impurities, and continual exposure of aggregate material. The difference in volume fraction of aggregate between the two concrete samples (57% and 69.6%) was reflected in the depth of affected (sublimated) material. Here, for the given conditions, it was predicted that 4.4 and 6.5 yr, respectively, would be needed to sublimate away a 1-cm-deep (0.4-in-deep) layer from the concrete samples. Sulfur sublimation rates were predicted to change dramatically over a temperature range from 15 to 120 °C (59 to 248 °F). Finally it was shown that the much lower vacuum on the Moon would contribute only slightly more to the sublimation rates determined from the ground-based experiments.

### 3. EXTREME COLD AND TEMPERATURE CYCLE CONSIDERATIONS REGARDING THE INTEGRITY AND COMPRESSION STRENGTH OF SULFUR CONCRETE

The previous section addressed the effect of sulfur sublimation in the hard vacuum that exists on the lunar surface and the consequence it could have if sulfur concrete were to be used as a construction material. It is obvious that sulfur concrete cannot be used in an environment where the temperature exceeds  $\approx 120\text{ }^{\circ}\text{C}$  ( $248\text{ }^{\circ}\text{F}$ )—sulfur’s melting temperature. It has also been shown that the sublimation rates below this temperature are relatively high and that a sulfur concrete product would quickly lose its integrity. On the other hand, at the lower lunar temperatures, e.g.,  $-180$  to  $-220\text{ }^{\circ}\text{C}$  ( $-292$  to  $-364\text{ }^{\circ}\text{F}$ ), the sublimation kinetics are so slow as to be essentially negligible. However, one must also consider the effects of such low temperatures and extreme temperature cycles on the mechanical properties of sulfur concrete, particularly as it is a composite material. The following subsections describe an effort to gain some insight regarding the mechanical properties of sulfur concrete that might be subjected to the extreme temperatures of the lunar environment.

#### 3.1 Experimental Procedure

The experimental procedure, for the most part, was described in section 2. Again, the same two compositions were employed: (1) Thirty-five wt. % pure sulfur with 65 wt. % JSC-1, and (2) a sulfur and silica binder mixture (25% sulfur and 20% silica by weight) with 55 wt. % JSC-1. The molten sulfur mixtures were cast into  $50.8\text{-mm}^3$  ( $2\text{-in}^3$ ) blocks and allowed to harden. A given block was then cut into eight  $25.4\text{-mm}$  ( $1\text{-in}$ ) cubes such as seen in figure 28. Blocks that showed significant imperfections such as large shrinkage cavities were discarded.

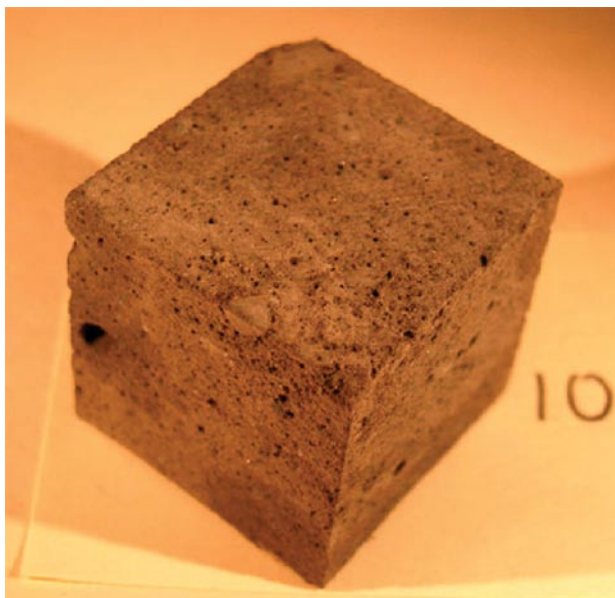


Figure 28. Typical  $2.54\text{-cm}$  ( $1\text{-in}$ ) cube of sulfur concrete used in this study. Sample composition is a silica binder mixture (25% sulfur and 20% silica by weight) with 55 wt. % JSC-1.

A set of eight cubes, four of each composition, was packaged with an enclosed k-type thermocouple and placed in the bottom of a wide mouth flexible plastic foam container into which liquid nitrogen (LN<sub>2</sub>) was poured. The container was capped with foam rubber, allowing the LN<sub>2</sub> to cool the samples and then evaporate over time. This cycle was repeated 80 times between RT ( $\approx 20$  °C, or 68 °F) and LN<sub>2</sub> ( $\approx -191$  °C, or  $-312$  °F) temperatures. A typical time-temperature plot is shown in figure 29.

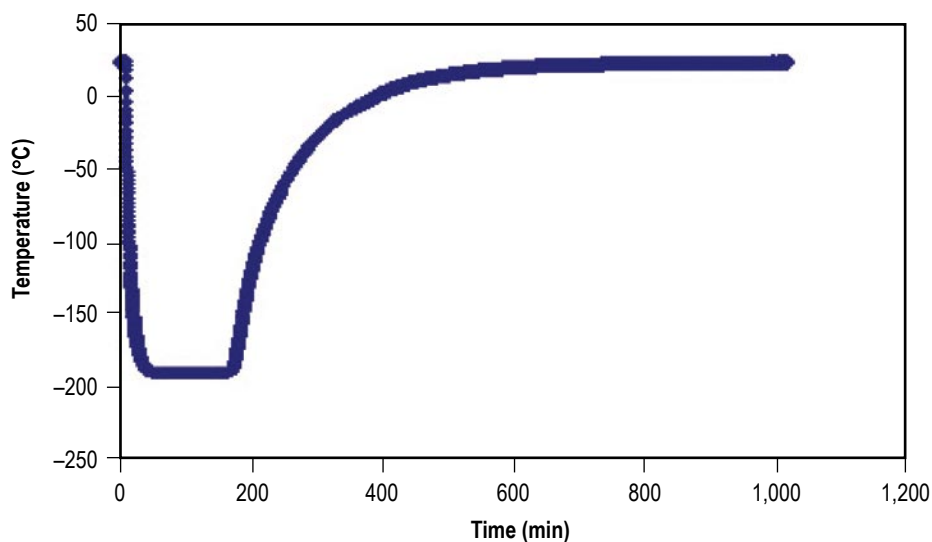


Figure 29. A typical time temperature plot showing one of the cycles the samples experienced.

Cycled and noncycled samples of both compositions were then subjected to compression testing at a constant downward crosshead speed of 0.127 cm/min (0.05 in/min). One set of samples was tested at room temperature ( $\approx 21$  °C, or 70 °F) and the other at  $\approx -101$  °C ( $\approx -150$  °F), figure 30. Compression data were gathered and the tests stopped after obvious crushing was observed.

### 3.2 Experimental Results

The noncycled samples were typical of that seen in figure 1, whereas those subjected to 80 cycles between RT and LN<sub>2</sub> temperatures exhibited cracking on the surface, such as seen in figure 31. The maximum strength achieved during compression testing of a given sample is shown in figure 32. Samples 1–16 were noncycled, whereas 17–24 were cycled. Information regarding sample composition and test temperature is located in the figure legend.

### 3.3 Discussion of Extreme Temperature Concerns

Consider first the noncycled samples, numbers 1–16. Samples 1–8 represent those consisting of sulfur - 65 wt. % JSC-1. The first four were tested at 21 °C (70 °F) and the latter four at  $-101$  °C ( $-150$  °F). Samples 9–16 represent the sulfur - 55 wt. % JSC-1 and 20 wt. % silica samples. Again, the first four were tested at 21 °C (70 °F) and the latter four at  $-101$  °C ( $-150$  °F). Looking at the group as a whole, the maximum compression ranges from  $\approx 17$  MPa to  $\approx 47$  MPa. In short, there are statistically insufficient data to make any conclusions regarding differences based on composition and/or test

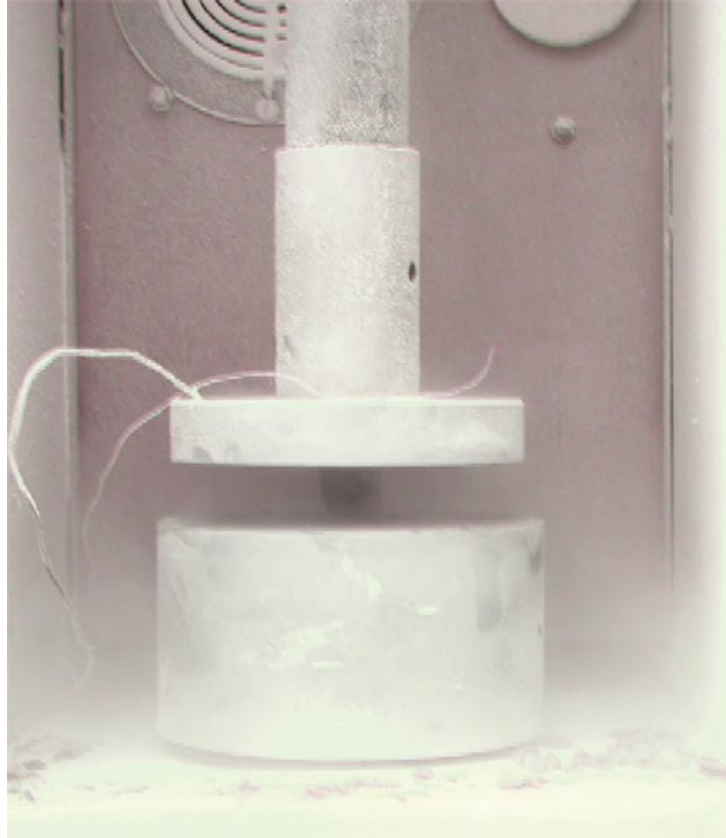


Figure 30. Photograph of a sample undergoing compression testing at  $-101\text{ }^{\circ}\text{C}$  ( $-150\text{ }^{\circ}\text{F}$ ).



Figure 31. Photograph of cracking exhibited on the surface of sample 22, which was subjected to 80 cycles between RT ( $\approx 21\text{ }^{\circ}\text{C}$ , or  $70\text{ }^{\circ}\text{F}$ ) and  $-191\text{ }^{\circ}\text{C}$  ( $-312\text{ }^{\circ}\text{F}$ ).

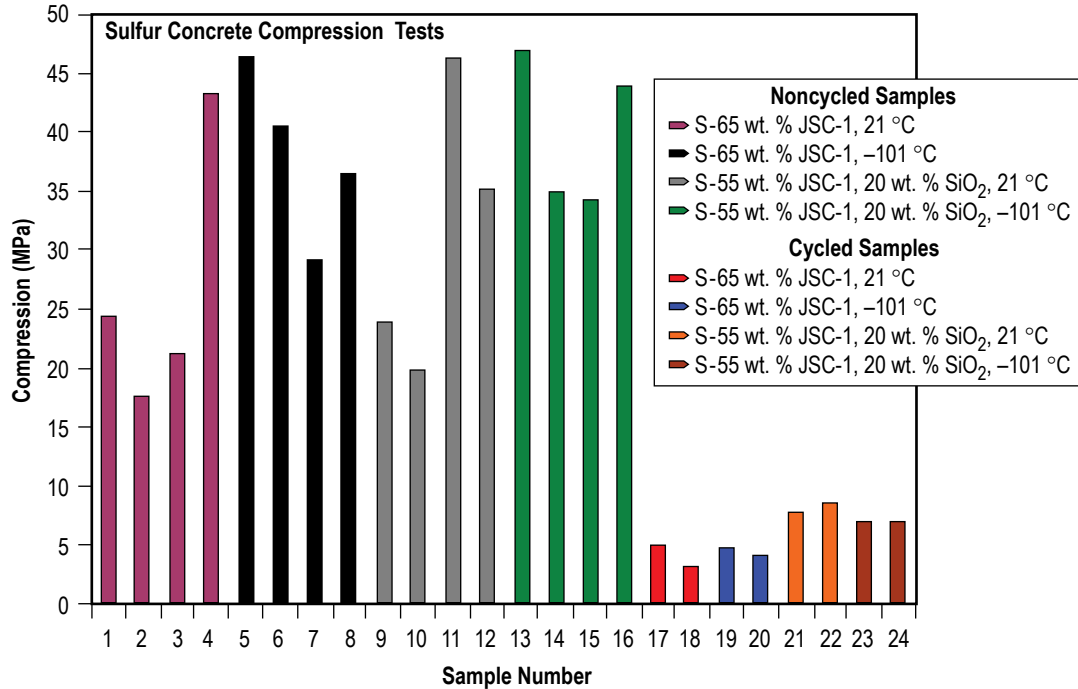


Figure 32. Plot of the maximum compression strength exhibited by the cycled and noncycled samples.

temperature. The discrepancy in results shown here is likely a consequence of defects such as inhomogeneous aggregate distribution and/or porosity that would arise during freezing of the concrete mixture.

The cycled samples, numbers 17–24, follow the same scenario as above, except that two instead of four samples per set were used. Here the test data range from  $\approx 3$  MPa to  $\approx 8$  MPa. Although the silica-containing samples appear to have performed slightly better, as one might intuitively think, there are no statistics to back that observation.

In summary, individual differences due to temperature or composition cannot be ascertained for either the cycled or noncycled sample groups. However, there is a clear difference between the maximum compression strength obtained from the cycled samples when compared to those noncycled samples. Assuming average compression failures of  $\approx 35$  MPa for the noncycled and  $\approx 7$  MPa for the cycled samples, a difference of about 5 times is seen, a factor that is easily attributed to the cracks observed on the cycled samples. This premise was investigated by examining the fracture surfaces and is best exemplified in the silica-containing samples.

Figures 33–36 are representative scanning electron micrographs of fracture surfaces from samples noted in figure 32. Figure 33 is taken from sample 10, a noncycled silica binder (25% sulfur and 20% silica by weight) with 55 wt. % JSC-1 mixture tested at 21 °C (70 °F). Figure 34 is from sample 14, which is like sample 10 in figure 33, but tested at  $-101$  °C ( $-150$  °F). Figure 35 is from sample 22, a cycled silica binder (25% sulfur and 20% silica by weight), with 55 wt. % JSC-1 mixture tested at 21 °C (70 °F). Figure 36 is from sample 24, which is like sample 22 in figure 35, but tested at  $-101$  °C ( $-150$  °F).

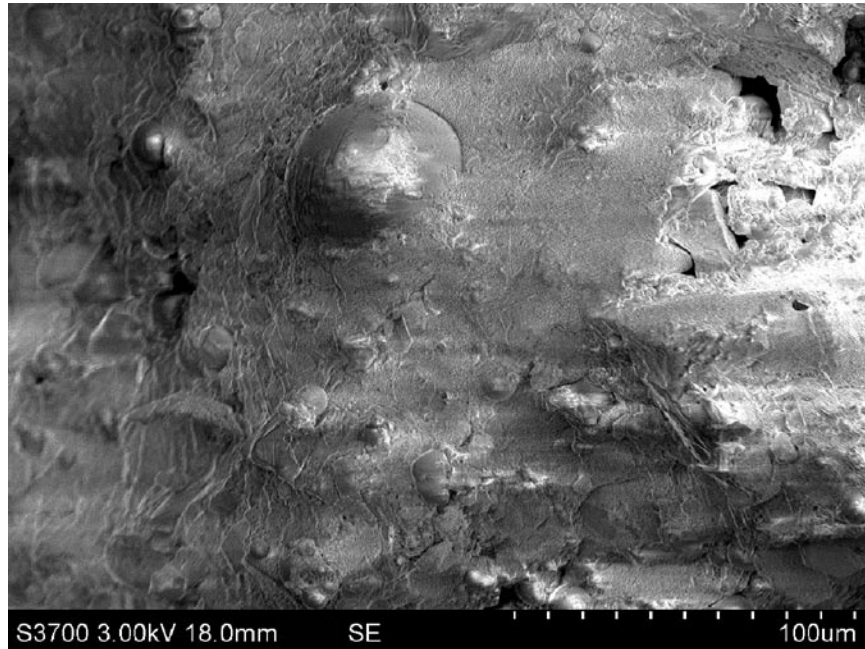


Figure 33. SEM micrograph of a fracture surface from noncycled sample 10, a silica binder mixture (25% sulfur and 20% silica by weight) with 55 wt. % JSC-1, tested at 21 °C (70 °F).

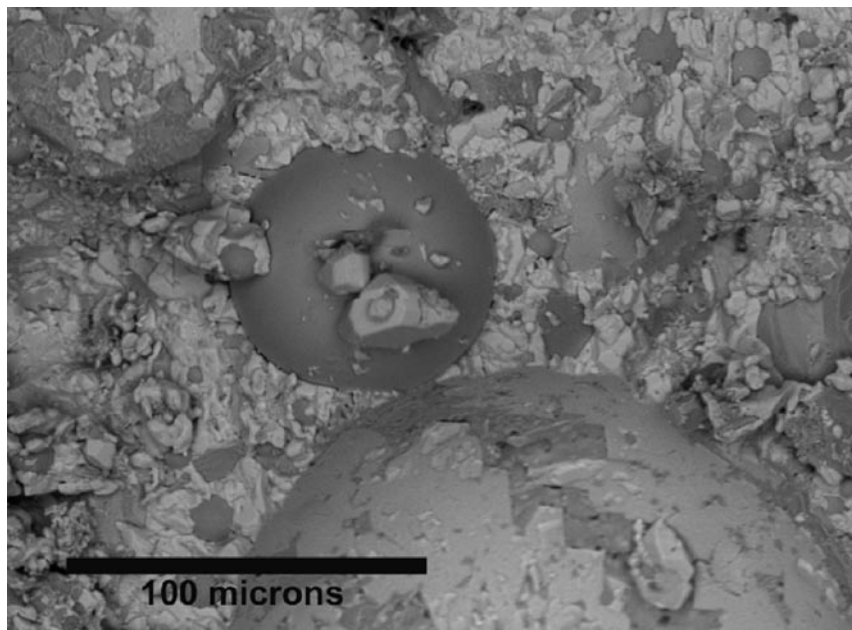


Figure 34. SEM micrograph of a fracture surface from noncycled sample 14, with the same composition as in figure 33, but tested at -101 °C (-150 °F).

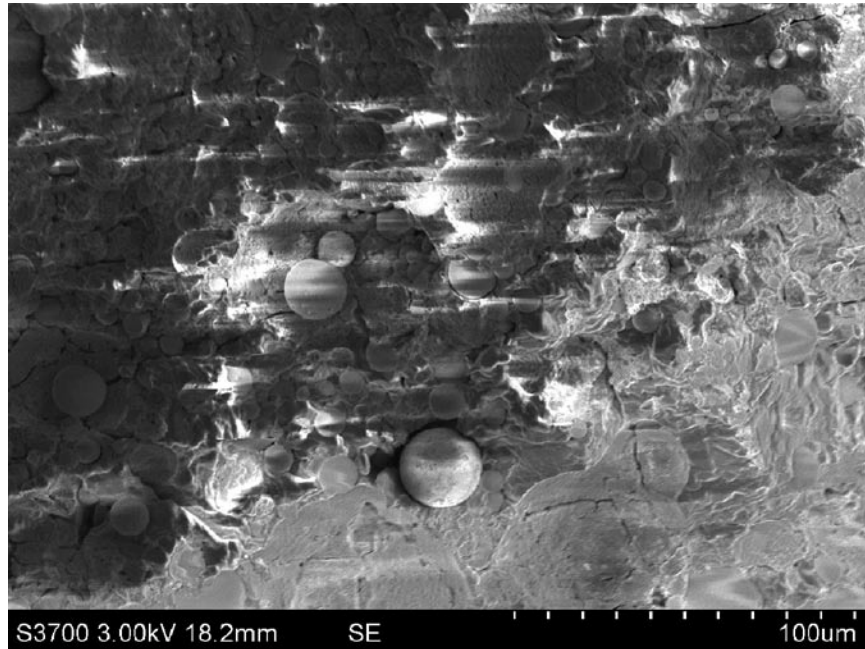


Figure 35. SEM micrograph of a fracture surface from cyclic sample 22, a silica binder mixture (25% sulfur and 20% silica by weight) with 55 wt. % JSC-1, tested at 21 °C (70 °F).

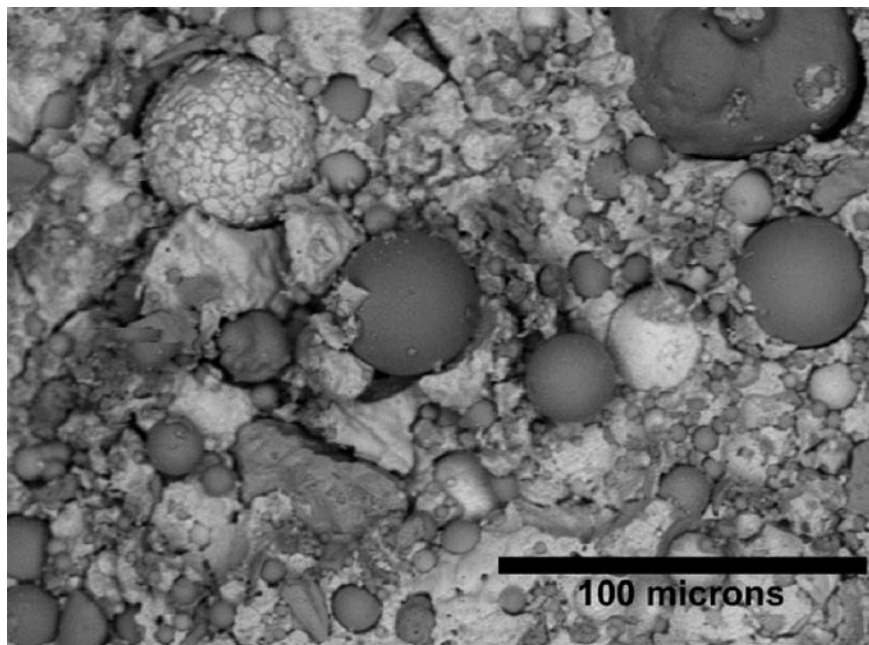


Figure 36. SEM micrograph of a fracture surface from cyclic sample 24, with the same composition as in figure 35, but tested at -101 °C (-150 °F).

Figure 33 is from noncycled sample 10 and shows a mottled fracture path through the sulfur and around the spherical silica particles. Note that the particles have maintained good coherency with the sulfur binder, some of which can be seen adhering to the surface of the large particle at the top center of the micrograph. Sample 10 also had one of the lowest compression strengths. This is likely due to porosity, as can be seen in the upper right hand corner, which was in evidence throughout this section. Sample 14 was tested at  $-101\text{ }^{\circ}\text{C}$  ( $-150\text{ }^{\circ}\text{F}$ ) and figure 34 shows the fracture surface morphology. Bonding of the silica particles with the sulfur is again evident, and the surface looks like that of figure 33, less the porosity; any distinction due to the lower test temperature is not obvious. Figure 35 is from cycled sample 22, tested at  $21\text{ }^{\circ}\text{C}$  ( $70\text{ }^{\circ}\text{F}$ ). Here, in contrast to figure 33, spherical silica particles are seen lying on the surface fully de-bonded from the sulfur binder. This is again seen in sample 24, figure 36.

Figures 37– 40 are representative scanning electron micrographs of fracture surfaces from the sulfur - 65 wt. % JSC-1 samples noted in figure 32. Figure 37 is taken from sample 4, a noncycled sample tested at  $21\text{ }^{\circ}\text{C}$  ( $70\text{ }^{\circ}\text{F}$ ). Figure 38 is from noncycled sample 6, which is like sample 4 in figure 37, but tested at  $-101\text{ }^{\circ}\text{C}$  ( $-150\text{ }^{\circ}\text{F}$ ). Figure 39 is from sample 18, a cycled sample tested at  $21\text{ }^{\circ}\text{C}$  ( $70\text{ }^{\circ}\text{F}$ ). Figure 40 is from sample 20, which is like sample 18 in figure 39, but tested at  $-101\text{ }^{\circ}\text{C}$  ( $-150\text{ }^{\circ}\text{F}$ ). Note that extensive cracking and de-bonding are also seen in the cycled 65 wt. % JSC-1 samples (figs. 39 and 40) when compared to those noncycled samples (figs. 37 and 38)—perhaps, though, not as simply observed as with the samples (figs. 35 and 36) containing the spherical silica particles.



Figure 37. SEM micrograph of a fracture surface from noncycled sample 4, a sulfur with 65 wt. % JSC-1 sample tested at  $21\text{ }^{\circ}\text{C}$  ( $70\text{ }^{\circ}\text{F}$ ).

As mentioned above, no conclusion on fracture strength could be determined as a function of composition or test temperature, yet the cycled samples failed at a load some 5 times less than the non-cycled. It appears obvious that this difference is due to de-bonding of the aggregate particles with the



Figure 38. SEM micrograph of a fracture surface from noncycled sample 6 with the same composition as in figure 37, but tested at  $-101\text{ }^{\circ}\text{C}$  ( $-150\text{ }^{\circ}\text{F}$ ).

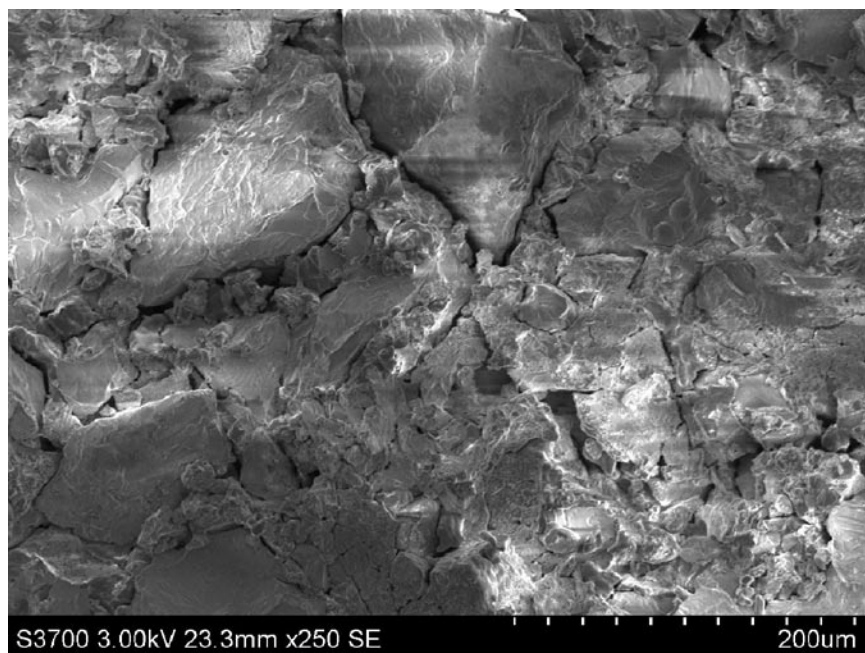


Figure 39. SEM micrograph of a fracture surface from cycled sample 18, a sulfur with 65 wt. % JSC-1 sample tested at  $21\text{ }^{\circ}\text{C}$  ( $70\text{ }^{\circ}\text{F}$ ).

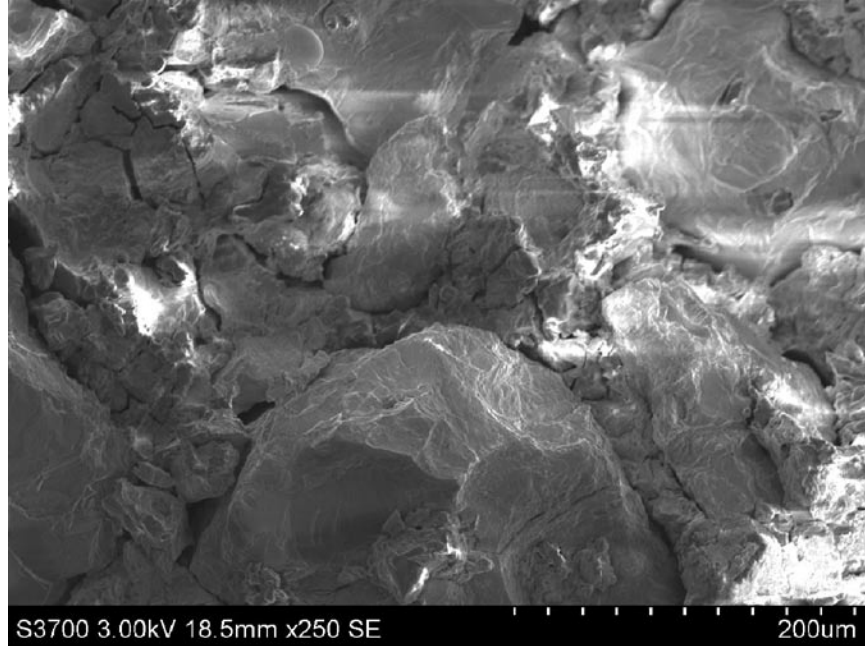


Figure 40. SEM micrograph of a fracture surface from cycled sample 20 with the same composition as figure 39, but tested at  $-101\text{ }^{\circ}\text{C}$  ( $-150\text{ }^{\circ}\text{F}$ ).

sulfur, essentially leaving a sample full of cracks prior to compression testing. Samples at  $-101\text{ }^{\circ}\text{C}$  ( $-150\text{ }^{\circ}\text{F}$ ) behaved like those tested at  $21\text{ }^{\circ}\text{C}$  ( $70\text{ }^{\circ}\text{F}$ ), but those tested at  $-191\text{ }^{\circ}\text{C}$  ( $-312\text{ }^{\circ}\text{F}$ ), and cycled, had inferior properties. One must now question if de-bonding is a consequence of temperature or cycling or both.

Sulfur is undoubtedly one of the most complex elements. It has numerous allotropic forms in the solid, liquid, and gaseous states, as noted earlier. Several slightly different pressure versus temperature phase diagrams have been published, and even its melting point still appears questionable. Consequently, the material properties of sulfur, particularly those at low temperatures, are less than well known. One can, however, make some assumptions in an attempt to shed light on the observations made above.

Chempruf Concrete<sup>1</sup> reports the coefficient of thermal expansion for their sulfur-based product to be  $\approx 1.2 \times 10^{-5}/\text{K}$  ( $6.67 \times 10^{-6}/\text{K}$ ). The coefficient of thermal expansion for  $\text{SiO}_2$  (silica), from  $527.7\text{ }^{\circ}\text{R}$  ( $20\text{ }^{\circ}\text{C}$ ) to  $1067.7\text{ }^{\circ}\text{R}$  ( $320\text{ }^{\circ}\text{C}$ ), is known to be  $5.5 \times 10^{-7}\text{ cm/cm K}$  ( $3.055 \times 10^{-7}/^{\circ}\text{R}$ ).<sup>44</sup> Sulfur and, essentially, silicates, compose the concrete; there is no chemically reacted bond between them; and there is a difference of two orders of magnitude in their coefficient of thermal expansion. The strain put on a material as a function of temperature can be evaluated as follows:

$$\varepsilon = \frac{\Delta L}{L} = \alpha \Delta T \quad . \quad (2)$$

Here  $\varepsilon$  is the strain,  $\Delta L$  is the change in the original length ( $L$ ),  $\alpha$  is the coefficient of thermal expansion, and  $\Delta T$  is the temperature difference that imposes the strain. For sulfur, cycling between  $21\text{ }^{\circ}\text{C}$  ( $70\text{ }^{\circ}\text{F}$ ) and  $-191\text{ }^{\circ}\text{C}$  ( $-312\text{ }^{\circ}\text{F}$ ) gives  $\Delta T = 216\text{ K}$  ( $381.6\text{ }^{\circ}\text{R}$ ), and the calculated strain would be

$2.6 \times 10^{-2}$ . The calculated strain in  $\text{SiO}_2$  is  $1.16 \times 10^{-4}$ , which is essentially negligible but important in the sense that two orders of magnitude exist between the materials. For metals, the generally accepted transition from elastic behavior to plastic behavior (permanent deformation) occurs at a strain of 0.002. Assuming this also applies to sulfur,  $\Delta T$  for the elastic-plastic transition would be  $\approx 167 \text{ K}$  ( $300.6 \text{ }^\circ\text{R}$ ) and from RT ( $21 \text{ }^\circ\text{C}$ ,  $69.8 \text{ }^\circ\text{F}$ ) corresponds to a temperature of approximately  $-146 \text{ }^\circ\text{C}$  ( $-230.8 \text{ }^\circ\text{F}$ ). This temperature appears reasonable, as an earlier study<sup>25</sup> cycled samples 50 times between RT and  $-27 \text{ }^\circ\text{C}$  ( $-16.6 \text{ }^\circ\text{F}$ ), with compression test results being similar to noncycled, RT samples. Though not cycled, samples compressed at  $-101 \text{ }^\circ\text{C}$  ( $-150 \text{ }^\circ\text{F}$ ) showed no discernible difference in properties or fracture microstructure from the strictly RT samples.

The data indicate that a transition occurred while cooling to  $-191 \text{ }^\circ\text{C}$  ( $-312 \text{ }^\circ\text{F}$ ), and a temperature of  $-146 \text{ }^\circ\text{C}$  ( $-230.8 \text{ }^\circ\text{F}$ ) was suggested. This value can only be considered an estimate, particularly in view of uncertain property values, especially at such low temperatures. Also likely is a functional relationship between temperature and the number of cycles needed to initiate and complete, or nearly complete, de-bonding; heating and cooling rates may also be a factor. Finally, it was assumed that the aggregate was pure  $\text{SiO}_2$ , when in reality  $\text{SiO}_2$  composed only  $\approx 20\%$ . The rest was JSC-1, a material composed of a number of minerals, albeit mostly silicates. These variables, including volume fraction of aggregate (as well as their size and shape), are all additionally influenced by the inherent sample inhomogeneities which further compromise accurately determining concrete viability. What does appear certain is that the contracting sulfur has a comparatively poor bond with the aggregate material and separates at that interface rather than fracturing within itself.

To gain some insight on cycling between room and  $\text{LN}_2$  temperatures, samples of sulfur with 65 wt. % pure  $\text{SiO}_2$  were made (a piece is seen in fig. 41), and placed in quartz test tubes. As expected, no integrity was lost when a sample was cycled 20 times between RT and  $-15 \text{ }^\circ\text{C}$  ( $5 \text{ }^\circ\text{F}$ ). However, debris was seen to accumulate after the seventh cycle for the sample tube immersed in  $\text{LN}_2$  ( $-196 \text{ }^\circ\text{C}$ , or  $-320.8 \text{ }^\circ\text{F}$ ). By the 20th cycle, the once solid piece had crumbled to free grains of  $\text{SiO}_2$  and small pieces of sulfur, as seen in figure 42. Here the only 'outside' forces experienced by the sample were gravity and slight movements due to manipulating the test tube. One also can assume that concrete integrity could be significantly compromised after the first cycle. In retrospect, cycling the samples 80 times was certainly excessive.

### 3.4 Summary of Extreme Temperature Concerns

Work was undertaken to evaluate the structural integrity of sulfur concrete that was subjected to cycling between temperatures that might be expected on the lunar surface. Previous work showed that the compression strength of samples cycled between RT and  $-27 \text{ }^\circ\text{C}$  ( $-16.6 \text{ }^\circ\text{F}$ ) was not statistically different from noncycled samples. In contrast, samples cycled between room temperature and  $-191 \text{ }^\circ\text{C}$  ( $-312 \text{ }^\circ\text{F}$ ) showed at least 5 times less strength than those noncycled. Microscopic investigation of the fracture surfaces showed clear de-bonding of  $\text{SiO}_2$  particles from the sulfur. The observed de-bonding is attributed to the large differences between the coefficients of expansion of sulfur and aggregate, and it initiates at some yet unknown temperature(s) where the induced strain is sufficient for the sulfur to go from elastic to plastic behavior. A simple test suggested that significant structural degradation initiates after only a few cycles between room and  $\text{LN}_2$  temperatures. While de-bonding and poor mechanical behavior are certain, a complete analysis is hampered by lacking material properties at low temperatures,

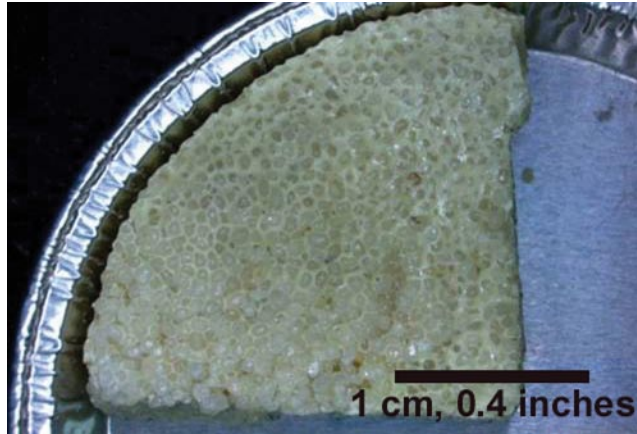


Figure 41. Photograph of a sulfur sample with 65 wt. % pure  $\text{SiO}_2$ .



Figure 42. Photograph of a sample like that seen in figure 7 which was cycled 20 times between room temperature and  $-196\text{ }^\circ\text{C}$  ( $-321\text{ }^\circ\text{F}$ ). Crumbling of the sample with free grains of silica is seen.

using partially characterized aggregate, and using samples that have inherent defects such as poor aggregate distribution and variable porosity. Such problems will likely be exacerbated if sulfur concrete is produced on the lunar surface.

#### 4. OVERALL SUMMARY AND CONCLUSIONS

Melting sulfur and mixing it with an aggregate to form ‘concrete’ is commercially well established and produces a material that is particularly well-suited for use in corrosive environments. Discovery of the mineral troilite (FeS) on the Moon poses the question of extracting the sulfur for use as a lunar construction material, an attractive alternative to conventional concrete as sulfur concrete does not require water. However, the viability of sulfur concrete in a lunar environment, which is characterized by the lack of an atmosphere and the presence of extreme temperatures, is not well understood. The intent of the work presented here was to conduct a series of ground-based experiments to gain insight regarding any detrimental effects that the extreme environmental conditions of the lunar surface might have on sulfur concrete. Here it is assumed that the lunar ore can be mined and refined and the raw sulfur melded with appropriate lunar regolith to form, for example, bricks.

The first issue addressed was the ‘hard’ vacuum environment of the lunar surface and how it might sublimate away exposed sulfur and degrade any concrete structure. In this study, small, pure sulfur and two sulfur ‘concrete’ mixtures were prepared and placed in a vacuum environment (capable of  $5 \times 10^{-7}$  torr) at  $\approx 20$  °C ( $\approx 68$  °F) for 60 days. Periodic weighing of the samples revealed a continuous weight loss due to the sublimation of sulfur. Reasonable agreement with the Hertz-Knudsen equation was seen over  $\approx 10$  days. Subsequent deviation was attributed to nonuniform surfaces, cavity formation, and increased exposure of aggregate material. The sublimation rate varied from rapid at the highest lunar temperatures expected to essentially nonexistent at the lowest.

Second, blocks of sulfur concrete were cycled between LN<sub>2</sub> temperature ( $\approx -191$  °C, or  $-312$  °F) and RT (18 to 20 °C, or 64.4 to 68 °F) to simulate exposure to the extreme cold of the lunar environment. These, and a similar set of blocks not cycled, were subsequently subjected to compression testing at two temperatures,  $\approx 21$  °C and  $\approx -101$  °C ( $\approx 70$  °F and  $\approx -150$  °F). No effect of the different compositions or test temperatures could be ascertained from either set. However, the compression strength of the noncycled samples averaged roughly 35 MPa ( $\approx 5,076$  psi), whereas the cycled samples fractured at about 7 MPa ( $\approx 1,015$  psi), or approximately one-fifth the load of noncycled samples. The disparity in strength was attributed to significant differences in thermal coefficients of expansion, which promoted cracking.

In short, ‘warm’ lunar temperatures maintain mechanical properties but increase sublimation kinetics, whereas ‘cold’ temperatures minimize sublimation effects but degrade mechanical properties. In conclusion, as on Earth, use of sulfur concrete in the lunar environment as a construction material will require special circumstances. Finally, it has been suggested that a ‘protective’ coating be put on the sulfur concrete. Perhaps, but first, issues of compatibility, safety, resources, and likely other concerns would have to be addressed.

## REFERENCES

1. GRC, Inc.-Chempruf, P.O. Box 644, Clarksville, TN 37040, <<http://www.chemproofconcrete.com>> Accessed 3 October 2007.
2. Sullivan, D.: "Acid-Proof Coating Composition," U.S. Patent No. 1,808,081, June 2, 1931.
3. Leutner, B.; and Diehl, L.: "Manufacture of Sulfur Concrete," U.S. Patent No. 4,025,352, May 24, 1977.
4. Vroom, A.H.: "Sulphur Cements, Process for Making Same and Sulphur Concretes Made Therefrom," U.S. Patent No. 4,058,500, November 15, 1977.
5. ACI Committee 548: "Guide for Mixing and Placing Sulfur Concrete in Construction," *ACI Materials Journal*, Farmington Hills, MI, p. 314, July–August, 1998.
6. Crick, S.M.; and Whitmore, D.W.: "Using Sulfur Concrete on a Commercial Scale," *Concrete International*, Vol. 20(2), p. 83, February 1998.
7. Czarnecji, B.; and Gillott, J.E.: "Effect of Different Admixtures on the Durability of Sulfur Concrete Made with Different Aggregates," *Engineering Geology*, Vol. 28(1–2), pp. 105–118, 1990.
8. Head, W. J.: "Fly Ash Sulfur Concrete," *Transportation Engineering Journal*, Vol. 107(3), pp. 345–363, May/June 1981.
9. Khalooand, A.R.; and Ghafouri, H.R.: "Parameters Influencing the Behavior of Sulfur Concrete," *Proc., Intern. Concrete Conf. 92*, Tehran, pp. 270–288, November 1992.
10. Lin, S-L; Lai, J.S.; and Chain, E.S.K.: "Modifications of Sulfur Polymer Cement (SPC) Stabilization and Solidification (S/S) Process," *Waste Management*, Vol. 15(5/6), pp. 441–447, 1995.
11. Loov, R.E.; Vroom, A.H.; and Ward M.A.: "Sulfur Concrete—A New Construction Material," *PCI Journal*, pp. 86–95, January–February 1974.
12. Hammons, M.I.; Smith, D.M.; Wilson, D.E.; and Reece, C.S.: "Investigation of Modified Sulfur Concrete as a Structural Material," U.S. Army Corps of Engineers, Technical Report CPAR-SL-93-1, July 1993.
13. Malhotra, V.M.: "Sulfur-Infiltrated Concrete," *Concrete Construction*, March 1975.
14. Okumura, H.A.: "Early Sulfur Concrete Installations," *Concrete International* 20, No. 1, p. 72, January 1998.

15. Nevin, P.J.: “Assessing Sulfur Concrete Applications,” *Concrete International* 20, No. 2, p. 87, February 1998.
16. Vroom, A.H.: “Sulfur Concrete Goes Global,” *Concrete International* 20, No. 1, p. 68, January 1998.
17. Vroom, A.H.: “Sulfur Concrete for Precast Products,” *Concrete International* 20, No. 2, p. 90, February 1998.
18. Taylor, G.J.; Warren, P.; Ryder, G.; Delano, J.; Pieters, C.; and Lofgren, G.: “Lunar Rocks,” *Lunar Sourcebook*, G.H. Heiken, D. Vaniman, and B.M. French (eds.), Cambridge University Press, pp. 183–284, 1991.
19. Haskin, L.; and Warren, P.: “Lunar Chemistry,” *Lunar Sourcebook*, G.H. Heiken, D. Vaniman, and B.M. French (eds.), Cambridge University Press, pp. 357–474, 1991.
20. Vaniman, D.; Pettit, D.; and Heiken, G.: “Uses of Lunar Sulfur,” *Second Conference on Lunar Bases and Space Activities of the 21st Century*, Wendell Mendell (ed.), Lunar and Planetary Institute, pp. 429–435, 1992.
21. Casanova, I.: “Feasibility and Applications of Sulfur Concrete for Lunar Base Development: A Preliminary Study,” *28th Annual Lunar and Planetary Science Conference, March 17–21, Houston, TX*, p. 209, 1997.
22. Gracia, V.; and Casanova, I.: “Sulfur Concrete: A Viable Alternative for Lunar Construction,” *Proceedings of the Sixth International Conference and Exposition on Engineering, Construction and Operations in Space, Albuquerque, New Mexico*, pp. 585–591, April 26–30, 1998.
23. Leonard, R.S.; and Johnson, S.W.: “Sulfur-Based Construction Materials for Lunar Construction,” *Engineering, Construction, and Operations in Space, Proc. of Space 88*, S.W. Johnson and J.P. Wetzel, ASCE (eds.), pp. 1295–1307, 1988.
24. Roqueta, J.; and Casanova, I.: “Manufacture and Properties of Sulfur Mortar for Lunar Applications,” *Proceedings of the 7th International Conference and Exposition on Engineering, Construction, Operations and Business in Space*, S.W. Johnson, K.M. Chua, R. Galloway, and P. Richter (eds.), Albuquerque, NM, pp. 851–855, 2000.
25. Toutanji, H.; Glenn-Loper, B.; and Schrayshuen, B.: “Strength and Durability Performance of Waterless Lunar Concrete,” AIAA proceedings paper No. 2005-1436.
26. Grugel, R.N.; and Toutanji, H.: “Viability of Sulfur ‘Concrete’ on the Moon: Environmental Considerations,” AIAA proceedings paper No. 2006-520, 2006.
27. Grugel, R.N.; and Toutanji, H.: “Sulfur ‘Concrete’ for Lunar Applications— Sublimation Concerns,” *Advances in Space Research*, Vol. 41, pp. 103–112, 2008.

28. Jones, L.; and Atkins, P: *Chemistry: Molecules, Matter and Change*, 4th ed., W.H. Freeman, New York, 2000.
29. Honig, R.E.; Kramer, D.A.: "Vapor Pressure Data for the Solid and Liquid Elements," *RCA Review*, Vol. 30, pp. 285–305, 1969.
30. McKay, D.S.; Carter, J.L.; Boles, W.W.; Allen, C.C.; and Allton, J.H.: "JSC-1: A New Lunar Soil Simulant," *Engineering, Construction, and Operations in Space IV*, American Society of Civil Engineers, pp. 857–866, 1994.
31. Hertz, H.: "Über die Verdunstung der Flüssigkeiten, insbesondere des Quecksilbers, im luftleeren Raume," *Ann. Physik*, Vol. 17, p. 177, 1882.
32. Knudsen, M.: "Die Molekularströmung der Gase durch Öffnungen und die Effusion," *Ann. Physik*, 4th series, Vol. 28, p. 999, 1909.
33. Langmuir, I.: "Chemical Reactions at Very Low Pressures. II. The Chemical Clean-up of Nitrogen in a Tungsten Lamp," *J. Am. Chem. Soc.*, Vol. 35, p. 931, 1913.
34. McEachern, D.M.; and Sandoval, O.: "A Molecular Flow Evaporating Apparatus for Measuring Vapour Pressures and Heats of Sublimation of Organic Compounds," *J. of Physics E: Scientific Instruments*, Vol. 6, pp. 155–161, 1973.
35. Langmuir, I.: "The Vapor Pressure of Metallic Tungsten," *Physical Review*, Vol. II(5) pp. 329–342, 1913.
36. Marshall, A.L.; Dornte, R.W.; Norton, F.J.: "The Vapor Pressure of Copper and Iron," *J. Amer. Chem. Soc.*, Vol. 59(7), pp. 1161–1166, 1937.
37. Johnston, H.L.; and Marshall, A.L.: "Vapor Pressures of Nickel and of Nickel Oxide," *J. Amer. Chem. Soc.*, Vol. 62, pp. 1382–1390, 1940.
38. Holden, R.B.; Speiser, R.; and Johnston, H.L.: "The Vapor Pressures of Inorganic Substances. I. Beryllium," *J. Amer. Chem. Soc.*, Vol. 70, pp. 3897–3899, 1948.
39. Rosenblatt, G.M.; and Lee, P-H.: "Vaporization Kinetics and Thermodynamics of Antimony and the Vaporization Coefficient of Antimony Single Crystals," *J. Chem. Phys.*, Vol. 52, pp. 1454–1464, 1970.
40. Howlett, D.L.; Lester, J.E.; and Somorjai, G.A.: "Vacuum Vaporization Studies of Lithium Fluoride Single Crystals," *J. Phys. Chem.*, Vol. 75, pp. 4049–4053, 1971.
41. Wang, L.L.; Wallace, T.C., Sr.; Hampel, F.G.; and Steele, J.H.: "Vacuum Evaporation of KCl-NaCl Salts: Part II. Vaporization-Rate Model and Experimental Results," *Met. and Mat. Trans. B 27B*, p. 657, 1996.

42. Rosenblatt, G.M.; and Lee, P-H.: "Rate of Vaporization of Arsenic Single Crystals and the Vaporization Coefficient of Arsenic," *J. Chem. Phys.*, Vol. 49, pp. 2995–3006, 1969.
43. Inaba, H.; Tachibana, S.; Nagahara, H.; and Ozawa, K.: "Condensation Kinetics of Forsterite," *Proceedings, Lunar and Planetary Science XXXII*, paper 1837, 2001.
44. Weast, R.C. (ed.): *Handbook of Chemistry and Physics*, 57th edition, CRC Press, 1976–1977.

## REPORT DOCUMENTATION PAGE

*Form Approved*  
OMB No. 0704-0188

Public reporting burden for this collection of information is estimated to average 1 hour per response, including the time for reviewing instructions, searching existing data sources, gathering and maintaining the data needed, and completing and reviewing the collection of information. Send comments regarding this burden estimate or any other aspect of this collection of information, including suggestions for reducing this burden, to Washington Headquarters Services, Directorate for Information Operation and Reports, 1215 Jefferson Davis Highway, Suite 1204, Arlington, VA 22202-4302, and to the Office of Management and Budget, Paperwork Reduction Project (0704-0188), Washington, DC 20503

<b>1. AGENCY USE ONLY</b> (Leave Blank)		<b>2. REPORT DATE</b> February 2008	<b>3. REPORT TYPE AND DATES COVERED</b> Technical Memorandum	
<b>4. TITLE AND SUBTITLE</b> Sulfur 'Concrete' for Lunar Applications—Environmental Considerations			<b>5. FUNDING NUMBERS</b>	
<b>6. AUTHORS</b> R.N. Grugel				
<b>7. PERFORMING ORGANIZATION NAME(S) AND ADDRESS(ES)</b> George C. Marshall Space Flight Center Marshall Space Flight Center, AL 35812			<b>8. PERFORMING ORGANIZATION REPORT NUMBER</b>  M-1223	
<b>9. SPONSORING/MONITORING AGENCY NAME(S) AND ADDRESS(ES)</b> National Aeronautics and Space Administration Washington, DC 20546-0001			<b>10. SPONSORING/MONITORING AGENCY REPORT NUMBER</b> NASA/TM—2008-215250	
<b>11. SUPPLEMENTARY NOTES</b> Prepared by the Materials and Processes Laboratory, Engineering Directorate				
<b>12a. DISTRIBUTION/AVAILABILITY STATEMENT</b> Unclassified-Unlimited Subject Category 29 Availability: NASA CASI 301-621-0390			<b>12b. DISTRIBUTION CODE</b>	
<b>13. ABSTRACT</b> (Maximum 200 words) Commercial use of sulfur 'concrete' on Earth is well established, particularly in corrosive, e.g., acid and salt, environments. Having found troilite (FeS) on the Moon raises the question of using extracted sulfur as a lunar construction material, an attractive alternative to conventional concrete as it does not require water. For the purpose of this Technical Memorandum, it is assumed that lunar ore is mined, refined, and the raw sulfur processed with appropriate lunar regolith to form, for example, bricks. With this stipulation, it is then noted that the viability of sulfur concrete in a lunar environment, which is characterized by lack of an atmosphere and extreme temperatures, is not well understood. The work presented here evaluates two sets of small sulfur concrete samples that have been prepared using JSC-1 lunar simulant as an aggregate addition. One set was subjected to extended periods in high vacuum to evaluate sublimation issues, and the other was cycled between room and liquid nitrogen temperatures to investigate their subsequent mechanical integrity. Results are presented from both investigations, discussed, and put into the context of the lunar environment.				
<b>14. SUBJECT TERMS</b> lunar environment, lunar processing, in situ resource utilization, sulfur, sulfur concrete, sublimation, compression testing, composites, lunar soil simulant			<b>15. NUMBER OF PAGES</b> 48	
			<b>16. PRICE CODE</b>	
<b>17. SECURITY CLASSIFICATION OF REPORT</b> Unclassified	<b>18. SECURITY CLASSIFICATION OF THIS PAGE</b> Unclassified	<b>19. SECURITY CLASSIFICATION OF ABSTRACT</b> Unclassified	<b>20. LIMITATION OF ABSTRACT</b> Unlimited	



National Aeronautics and  
Space Administration  
IS20

**George C. Marshall Space Flight Center**  
Marshall Space Flight Center, Alabama  
35812